Int. J. Solids Structures Vol. 15, pp. 805–827
Pergamon Press Ltd., 1979. Printed in Great Britain

STRESS ANALYSIS FOR AN ELASTIC HALF SPACE CONTAINING AN AXIALLY-LOADED RIGID CYLINDRICAL ROD

V. K. LUK† and L. M. KEER

Department of Civil Engineering, Northwestern University, Evanston, IL 60201, U.S.A.

(*Received* 20 *July* 1978; *in revised form* 26 *February* 1979)

Abstract—The axially symmetric elastostatic problem of a half space containing a partially embedded, axially-loaded, rigid cylindrical rod is investigated. The rod is assumed to be in bonded contact with the half space and the half space surface is perpendicular to its axis. The problem is formulated by means of Hankel integral transforms and reduced to systems of coupled singular integral equations, where the unknown quantities are the normal and the shear stresses acting on the entire surface of the rod. Numerical solutions are obtained for several values of the aspect ratio, i.e. of radius to length, and for sufficiently small values of this ratio the results appear to be comparable to those of Muki and Sternberg for an axially-loaded rod. Comparison is also made for the percentage of the vertical resultant load carried by the base of rod with the results obtained by Poulos and Davis for a single axially-loaded incompressible pile.

1. INTRODUCTION

The diffusion of load from a bar into a three dimensional elastic medium presents considerable analytical difficulties and it is only recently that such problems have been solved, although the solutions generally involved approximations of various types. Poulos and Davis[1] using Mindlin's solution[2] as a basis, solved the pile problem in an approximate manner by integrating vertical forces along the depth and around the circumference of a cylindrical element. The force intensities were adjusted at discrete points to satisfy the boundary condition of prescribed vertical displacement. In this manner the effect of the length to diameter ratio upon the shear stress distribution and the proportion of the total load carried by the base could be estimated. This analysis has several limitations, the major ones being the absence of circumferential normal stresses on the cylinder wall and of shear stresses on the cylinder base and the neglect of compatibility of radial displacement on the cylinder wall.

Muki and Sternberg[3] investigated the diffusion of an axial load from an elastic rod of uniform cross section embedded in and bonded to an elastic half space. Their approximate method, which was also developed from Mindlin's solution and which required the length of the rod to be large in comparison to its diameter, led to a Fredholm integral equation. The accuracy of their solution was checked by applying their approximate technique to the exactly solved problem of an infinite bar embedded within an infinitely extended elastic medium[4]. The accuracy provided by this test solution gave good confidence in the accuracy of their load transfer problem, provided that their assumptions were met.

A recent paper by Suriyamongkal *et al.*[5] investigated the stress distribution and load transfer behavior of piles and caissons under vertical load by using a method analogous to that of Harding and Sneddon[6] to develop radial and vertical ring forces acting in the interior of a half space. Once the transforms appropriate for their solutions were developed, they then matched the appropriate boundary conditions to solve the problem of a rigid cylindrical body embedded within an elastic half space. It should be noted that although their results appear to differ from those of Muki and Sternberg, the latter's results would have to be extrapolated for the case that the rod is rigid. It is most likely that such an extrapolation might provide closer results between the two solutions.

The present analysis investigates the diffusion of load from a cylindrical rod into an elastic half space. The analysis, in principle, is somewhat similar to that of Poulos and Davis, except

†Present address: Stress Analyst, Joseph Oat Corporation, Camden, NJ 08104, U.S.A.

that Hankel integral transforms are used as a starting point and the technique of superposition of solutions is employed to obtain the desired solution. First, a problem for a rigid, cylindrical shell is formulated by appropriately using elastostatic solutions for a cylinder and for a cylindrical cavity with suitable matching conditions. Next, a solution is derived for a rigid circular plate parallel to and below the surface of an elastic half space. The superposition of the shell and the plate solutions leads to the establishment of systems of coupled singular integral equations in terms of unknown stress jumps over the entire surface of the cylindrical rod. The problems are formulated within the scope of the linear theory of elasticity, and isotropy and homogeneity of the elastic half space are assumed.

The three dimensional problems of this kind, which utilize the technique of superposition of solutions for a cylinder and a cylindrical cavity, require special analytical treatment if a stress free half space surface is desired. The formulation of the problem is unavoidably complicated to a great extent and the analytical difficulties so raised will be discussed in the next section. In similar two dimensional elasticity problems (see, e.g. Haritos and Keer[7]), the problem can be readily formulated to lead to a system of singular integral equations, having (in addition to the usual Cauchy kernels) kernels which are rational functions.

The numerical integration scheme described in a paper by Erdogan *et al.*[8] is used to obtain numerical solution. The percentage of the vertical resultant load carried by the base of rod for various values of aspect ratio is compared with that obtained by Poulos and Davis. The vertical displacement of the cylindrical structures which will in turn determine the compliance of the physical system under consideration is also calculated. Comparison of load transfer is also made with the Muki and Sternberg solution when the rod has an embedded length that is long compared to its radius.

2. RIGID CYLINDRICAL SHELL-PRELIMINARY PROBLEM

This portion of the analysis considers a single rigid cylindrical shell of radius c and height h with negligible thickness, partially embedded in an elastic half space. A cylindrical coordinate system (r, θ, z) is used with the z-axis coinciding with the axis of the shell, as shown in Fig. 1. The shell is perpendicular to the surface of half space and occupies the region $r = c$, $0 \le z \le h$. A solution is sought for the case that the cylindrical shell is subjected to a vertical load, $-T$; the surface of the half space is stress free.

The title problem will be formulated in Section 3 by considering the additional complication of a rigid disk, attached to the lower end of the shell; the elastic material contained within the shell end disk will move as a rigid body. For the shell porblem, elasticity solutions will be developed for two regions: region (1), a semi-infinite cylinder of radius c, and region (2), a half space having a cylindrical cavity of radius c. The rigid shell is common to both of these regions. The displacement continuity and boundary conditions, expressed in terms of cylindrical coordinates, are written as follows:

$$u_z^1 = u_z^2, \qquad r = c, \quad 0 \le z < \infty \tag{2.1}$$

$$u_r^1 = u_r^2, \tag{2.2}$$

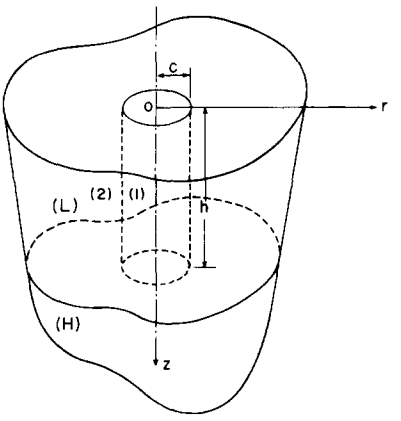

Fig. 1. Geometry and coordinate system of the shell and the rod.

$$\tau_{zr}^1 = \tau_{zr}^2 = 0, \qquad 0 \le r < \infty, \quad z = 0 \tag{2.3}$$

$$\tau_{zz}^1 = \tau_{zz}^2 = 0, \tag{2.4}$$

where u_z, u_r and τ_{zr}, τ_{zz}, τ_{rr} are displacements and stresses, assuming axial symmetry. In addition to the continuity and boundary conditions, the shell is required to displace as a rigid body in an axial direction, i.e.

$$\frac{\partial u_z}{\partial z} = 0, \qquad r = c, \quad 0 \le z \le h. \tag{2.5}$$

$$\frac{\partial u_r}{\partial z} = 0, \tag{2.6}$$

In addition, one must have an equation that gives the total load (overall equilibrium) and one that fixes the radial displacement; the two equations are to be used later as subsidiary conditions for the developed singular integral equations.

It is natural to express the displacements and stresses in terms of Hankel integral transforms for the two regions. The form of their representation is chosen to conveniently obtain a reduction to singular integral equations.

Region (1): $(0 \le r \le c, 0 \le z < \infty)$

$$2\mu u_z^1 = \int_0^\infty A(\xi)(1 - 2\nu + \xi z)\, e^{-\xi z} J_0(\xi r)\, d\xi - \int_0^\infty \xi [B_1(\xi) r I_1(\xi r) - B_2(\xi) I_0(\xi r)] \cos(\xi z)\, d\xi \tag{2.7}$$

$$2\mu u_r^1 = -\int_0^\infty A(\xi)(2 - 2\nu - \xi z)\, e^{-\xi z} J_1(\xi r)\, d\xi + \int_0^\infty \{B_1(\xi)[4(1-\nu) I_1(\xi r) - \xi r I_0(\xi r)] + \xi B_2(\xi) I_1(\xi r)\} \sin(\xi z)\, d\xi \tag{2.8}$$

$$\tau_{zz}^1 = -\int_0^\infty \xi^2 z A(\xi)\, e^{-\xi z} J_0(\xi r)\, d\xi + \int_0^\infty \xi \{B_1(\xi)[2\nu I_0(\xi r) + \xi r I_1(\xi r)] - \xi B_2(\xi) I_0(\xi r)\} \sin(\xi z)\, d\xi \tag{2.9}$$

$$\tau_{zr}^1 = \int_0^\infty \xi A(\xi)\, e^{-\xi z}(1 - \xi z) J_1(\xi r)\, d\xi + \int_0^\infty \xi \{B_1(\xi)[2(1-\nu) I_1(\xi r) - \xi r I_0(\xi r)] + \xi B_2(\xi) I_1(\xi r)\} \cos(\xi z)\, d\xi \tag{2.10}$$

$$\tau_{rr}^1 = \int_0^\infty \xi A(\xi)\, e^{-\xi z}\left[(-2 + \xi z) J_0(\xi r) + (2 - 2\nu - \xi z)\frac{J_1(\xi r)}{\xi r}\right] d\xi + \int_0^\infty \xi \left\{ B_1(\xi)\left[(3 - 2\nu) I_0(\xi r) - (4 - 4\nu + \xi^2 r^2)\frac{I_1(\xi r)}{\xi r}\right] + \xi B_2(\xi)\left[I_0(\xi r) - \frac{I_1(\xi r)}{\xi r}\right]\right\} \sin(\xi z)\, d\xi. \tag{2.11}$$

Region (2): $(c \le r < \infty, 0 \le z < \infty)$

$$u_z^2 = \int_0^\infty A(\xi)(1 - 2\nu + \xi z)\, e^{-\xi z} J_0(\xi r)\, d\xi - \int_0^\infty \xi [C_1(\xi) r K_1(\xi r) - C_2(\xi) K_0(\xi r)] \cos(\xi z)\, d\xi \tag{2.12}$$

$$u_r^2 = -\int_0^\infty A(\xi)(2 - 2\nu - \xi z)\, e^{-\xi z} J_1(\xi r)\, d\xi + \int_0^\infty \{C_1(\xi)[4(1-\nu) K_1(\xi r) + \xi r K_0(\xi r)] - \xi C_2(\xi) K_1(\xi r)\} \sin(\xi z)\, d\xi \tag{2.13}$$

$$\tau_{zz}^2 = -\int_0^\infty \xi^2 z A(\xi)\, e^{-\xi z} J_0(\xi r)\, d\xi + \int_0^\infty \xi \{C_1(\xi)[-2\nu K_0(\xi r) + \xi r K_1(\xi r)] - \xi C_2(\xi) K_0(\xi r)\} \sin(\xi z)\, d\xi \tag{2.14}$$

$$\tau_{zr}^2 = \int_0^\infty \xi A(\xi)\, e^{-\xi z}(1-\xi z)J_1(\xi r)\, d\xi + \int_0^\infty \xi\{C_1(\xi)[2(1-\nu)K_1(\xi r) + \xi r K_0(\xi r)] - \xi C_2(\xi)K_1(\xi r)\}\cos(\xi z)\, d\xi \quad (2.15)$$

$$\tau_{rr}^2 = \int_0^\infty \xi A(\xi)\, e^{-\xi z}\left[(-2+\xi z)J_0(\xi r) + (2-2\nu-\xi z)\frac{J_1(\xi r)}{\xi r}\right] d\xi + \int_0^\infty \xi\left\{-C_1(\xi)\left[(3-2\nu)K_0(\xi r) + (4-4\nu+\xi^2 r^2)\frac{K_1(\xi r)}{\xi r}\right] + \xi C_2(\xi)\left[K_0(\xi r) + \frac{K_1(\xi r)}{\xi r}\right]\right\}\sin(\xi z)\, d\xi \quad (2.16)$$

where J_0, J_1, I_0, I_1, K_0, and K_1 represent the usual Bessel functions, and ν, μ are Poisson's ratio and shear modulus, respectively. It is clear from the form of eqns (2.7)–(2.16) that $A(\xi)$ is an integral transform appropriate to half space region while $B_i(\xi)$ and $C_i(\xi)$, $i = 1,2$ are integral transforms appropriate to cylinder and cylindrical cavity regions, respectively.

It can be seen that eqn (2.4) requiring zero normal stress on the surface of the half space is automatically satisfied in both regions. With the aid of the displacement continuity conditions in eqns (2.1) and (2.2), τ_{zr}^1 and τ_{rr}^1 can be expressed in terms of $A(\xi)$, $C_1(\xi)$ and $C_2(\xi)$ as follows:

$$\tau_{zr}^1 = \int_0^\infty \xi A(\xi)\, e^{-\xi z}(1-\xi z)J_1(\xi c)\, d\xi - \int_0^\infty \frac{\xi}{\Delta(\xi)}[C_1(\xi)\alpha(\xi) + \xi C_2(\xi)\beta(\xi)]\cos(\xi z)\, d\xi, \quad r = c, \quad 0 \le z < \infty \quad (2.17)$$

$$\tau_{rr}^1 = \int_0^\infty \xi A(\xi)\, e^{-\xi z}\left[(-2+\xi z)J_0(\xi c) + (2-2\nu-\xi z)\frac{J_1(\xi c)}{\xi c}\right] d\xi + \int_0^\infty \frac{\xi}{\Delta(\xi)}[C_1(\xi)\gamma(\xi) + \xi C_2(\xi)\delta(\xi)]\sin(\xi z)\, d\xi, \quad r = c, \quad 0 \le z < \infty \quad (2.18)$$

where

$$\Delta(\xi) = 4(1-\nu)I_0 I_1 - \xi c(I_0^2 - I_1^2) \quad (2.19)$$

$$\alpha(\xi) = \xi^2 c^2(I_0^2 - I_1^2)K_0 + 2(1-\nu)[\xi c(I_0^2 - I_1^2)K_1 + \xi c(I_0 K_1 - I_1 K_0)I_0 - 4(1-\nu)I_0 I_1 K_1] \quad (2.20)$$

$$\beta(\xi) = -\xi c(I_0^2 - I_1^2)K_1 + 2(1-\nu)I_1(I_0 K_1 - I_1 K_0) \quad (2.21)$$

$$\gamma(\xi) = \xi^2 c^2(I_0^2 - I_1^2)K_1 + \xi c(I_0^2 - I_1^2)K_0 + 2(1-\nu)\xi c I_0(I_0 K_0 - I_1 K_1) + 4(1-\nu)[(3-2\nu)I_0^2 K_1 - I_1(I_0 K_0 + I_1 K_1)] - \frac{16(1-\nu)^2}{\xi c} I_0 I_1 K_1 \quad (2.22)$$

$$\delta(\xi) = -\xi c(I_0^2 - I_1^2)K_0 - (I_0^2 - I_1^2)K_1 - 2(1-\nu)I_0(I_0 K_1 - I_1 K_0) + \frac{4(1-\nu)}{\xi c} I_0 I_1 K_1 \quad (2.23)$$

and

$$I_0 = I_0(\xi c), \quad I_1 = I_1(\xi c); \quad K_0 = K_0(\xi c), \quad K_1 = K_1(\xi c). \quad (2.24)$$

It is convenient to introduce the following definition of the jumps in stresses across the shell surface:

$$\phi(z) = \tau_{zr}^1 - \tau_{zr}^2; \quad \psi(z) = \tau_{rr}^1 - \tau_{rr}^2, \quad r = c, \quad 0 \le z \le h. \quad (2.25)$$

Through the application of Fourier sine and cosine transforms, it can be shown that

$$\tau_{zr}^1 = \int_0^\infty \xi A(\xi)\, e^{-\xi z}(1-\xi z)J_1(\xi r)\, d\xi + \frac{1}{\pi(1-\nu)}\int_0^h \phi(s)\, ds \int_0^\infty \xi c\{\xi r I_0(\xi r)K_0 + I_1(\xi r)[2(1-\nu)K_0 - \xi c K_1]\}\cos(\xi z)\cos(\xi s)\, d\xi + \frac{1}{\pi(1-\nu)}\int_0^h \psi(s)\, ds \int_0^\infty \xi c\{-\xi r I_0(\xi r)K_1 + I_1(\xi r)[2(1-\nu)K_1 + \xi c K_0]\}\cos(\xi z)\sin(\xi s)\, d\xi \quad (2.26)$$

$$\tau_{zr}^2 = \int_0^\infty \xi A(\xi)\, e^{-\xi z}(1-\xi z)J_1(\xi r)\,d\xi + \frac{1}{\pi(1-\nu)}\int_0^h \phi(s)\,ds \int_0^\infty \xi c\{\xi r I_0 K_0(\xi r) - [2(1-\nu)I_0 + \xi c I_1]K_1(\xi r)\}\cos(\xi z)\cos(\xi s)\,d\xi + \frac{1}{\pi(1-\nu)}\int_0^h \psi(s)\,ds \int_0^\infty \xi c\{\xi r I_1 K_0(\xi r) + [2(1-\nu)I_1 - \xi c I_0]K_1(\xi r)\}\cos(\xi z)\sin(\xi s)\,d\xi. \tag{2.27}$$

The boundary conditions described in eqn (2.3) require that the shear stress be zero at the surface of the half space, $z = 0$. This task is difficult, in general, because of the different expressions of shear stress given by eqns (2.26) and (2.27). For this reason it is convenient to give $A(\xi)$ the following definition:

$$A(\xi) = \sqrt{\frac{\pi}{2}}\int_0^c \xi^{1/2}\eta(\tau)J_{3/2}(\xi\tau)\,d\tau + \sqrt{\frac{\pi}{2}}\int_c^\infty \xi^{1/2}\lambda(\tau)J_{1/2}(\xi\tau)\,d\tau \tag{2.28}$$

where it is noted that, e.g.

$$\int_0^\infty \xi A(\xi)J_1(\xi r)\,d\xi = \frac{1}{r^2}\frac{d}{dr}\int_0^r \frac{\tau^{3/2}\eta(\tau)\,d\tau}{\sqrt{(r^2-\tau^2)}} - \frac{d}{dr}\int_r^\infty \frac{\tau^{-1/2}\lambda(\tau)\,d\tau}{\sqrt{(\tau^2-r^2)}}, \quad 0<r<\infty. \tag{2.29}$$

The foregoing equation appears in different forms in regions (1) and (2) because of the domains of definition of $\eta(\tau)$ and $\lambda(\tau)$ introduced in eqn (2.28), i.e.

$$\int_0^\infty \xi A(\xi)J_1(\xi r)\,d\xi = \frac{1}{r^2}\frac{d}{dr}\int_0^r \frac{\tau^{3/2}\eta(\tau)\,d\tau}{\sqrt{(r^2-\tau^2)}} - r\int_c^\infty \frac{\tau^{-1/2}\lambda(\tau)\,d\tau}{(\tau^2-r^2)^{3/2}}, \quad 0<r<c \tag{2.30}$$

$$\int_0^\infty \xi A(\xi)J_1(\xi r)\,d\xi = -\frac{d}{dr}\int_r^\infty \frac{\tau^{-1/2}\lambda(\tau)\,d\tau}{\sqrt{(\tau^2-r^2)}} - \frac{1}{r}\int_0^c \frac{\tau^{3/2}\eta(\tau)\,d\tau}{(r^2-\tau^2)^{3/2}}, \quad c<r<\infty. \tag{2.31}$$

It is convenient to introduce an additional solution with zero surface normal stress and with the surface shear stress equal to the negative of the second terms in eqns (2.30) and (2.31), i.e.

$$\tau_{zr}^a = \begin{cases} r\displaystyle\int_c^\infty \frac{\tau^{-1/2}\lambda(\tau)\,d\tau}{(\tau^2-r^2)^{3/2}}, & 0\le r<c,\ z=0 \\ \dfrac{1}{r}\displaystyle\int_0^c \frac{\tau^{3/2}\eta(\tau)\,d\tau}{(r^2-\tau^2)^{3/2}}, & c<r<\infty,\ z=0. \end{cases} \tag{2.32}$$

Thus an additional displacement field must be incorporated to obtain the desired solution, i.e.

$$2\mu u_z^a = \int_0^\infty \bar{A}(\xi)\left[\frac{1}{2}(\kappa-1)+\xi z\right]e^{-\xi z}J_0(\xi r)\,d\xi, \quad 0\le r<\infty,\ 0\le z<\infty \tag{2.33}$$

$$2\mu u_r^a = -\int_0^\infty \bar{A}(\xi)\left[\frac{1}{2}(\kappa+1)-\xi z\right]e^{-\xi z}J_1(\xi r)\,d\xi, \quad 0\le r<\infty,\ 0\le z<\infty \tag{2.34}$$

where

$$\kappa = 3-4\nu \tag{2.35}$$

$$\bar{A}(\xi) = \int_0^c\int_c^\infty \frac{u^2 J_1(\xi u)\tau^{-1/2}\lambda(\tau)}{(\tau^2-u^2)^{3/2}}\,d\tau\,du + \int_c^\infty\int_0^c \frac{J_1(\xi u)\tau^{3/2}\eta(\tau)}{(u^2-\tau^2)^{3/2}}\,d\tau\,du. \tag{2.36}$$

With this addition, eqns (2.26) and (2.27) can be evaluated on $z = 0$ in the form of Abel's integral equation, which can be solved for $\eta(\tau)$ and $\lambda(\tau)$ as follows:

$$\tau^{1/2}\eta(\tau) = \frac{8c}{\pi^2(\kappa+1)}\left\{\int_0^h \phi(s)S_1(s,\tau)\,ds + \int_0^h \psi(s)S_2(s,\tau)\,ds\right\} \tag{2.37}$$

$$\tau^{-1/2}\lambda(\tau)=\frac{4c}{\pi(\kappa+1)}\left\{\int_0^h \phi(s)S_3(s,\tau)\,ds+\int_0^h \psi(s)S_4(s,\tau)\,ds\right\} \tag{2.38}$$

where

$$S_1(s,\tau)=\int_0^\infty \frac{1}{\xi}\left\{\left[\left(\frac{1}{2}(\kappa-1)-\xi^2\tau^2\right)K_0-\xi cK_1\right]\sinh(\xi\tau)-\xi\tau\left[\frac{1}{2}(\kappa-1)K_0-\xi cK_1\right]\cosh(\xi\tau)\right\}\cos(\xi s)\,d\xi \tag{2.39}$$

$$S_2(s,\tau)=\int_0^\infty \frac{1}{\xi}\left\{\left[\left(\frac{1}{2}(\kappa+3)+\xi^2\tau^2\right)K_1+\xi cK_0\right]\sinh(\xi\tau)-\xi\tau\left[\frac{1}{2}(\kappa+3)K_1+\xi cK_0\right]\cosh(\xi\tau)\right\}\sin(\xi s)\,d\xi \tag{2.40}$$

$$S_3(s,\tau)=\int_0^\infty \left[\frac{1}{2}(\kappa+1)I_0-\xi\tau I_0+\xi cI_1\right]e^{-\xi\tau}\cos(\xi s)\,d\xi \tag{2.41}$$

$$S_4(s,\tau)=\int_0^\infty \left[-\frac{1}{2}(\kappa+1)I_1-\xi\tau I_1+\xi cI_0\right]e^{-\xi\tau}\sin(\xi s)\,d\xi. \tag{2.42}$$

The additional complexity in adding the displacement field, $\underline{u}^a$, is offset by the convenience of expressing $\eta(\tau)$ and $\lambda(\tau)$ as in eqns (2.37) and (2.38).

The displacements along the cylindrical shell surface, $r=c$, after some manipulations can be expressed in the following form (note that $\underline{u}^1=\underline{u}^2$):

$$\begin{aligned}2\mu u_z=&\sqrt{\frac{\pi}{2}}\int_0^c \eta(\tau)\,d\tau\int_0^\infty \xi^{1/2}\left[\frac{1}{2}(\kappa-1)+\xi z\right]e^{-\xi z}J_0(\xi c)J_{3/2}(\xi\tau)\,d\xi\\&+\sqrt{\frac{\pi}{2}}\int_c^\infty \lambda(\tau)\,d\tau\int_0^\infty \xi^{1/2}\left[\frac{1}{2}(\kappa-1)+\xi z\right]e^{-\xi z}J_0(\xi c)J_{1/2}(\xi\tau)\,d\xi\\&+\frac{4c}{\pi(\kappa+1)}\int_0^h \phi(s)\,ds\int_0^\infty [(\kappa+1)I_0K_0-\xi c(I_0K_1-I_1K_0)]\cos(\xi z)\cos(\xi s)\,d\xi\\&+\frac{4c}{\pi(\kappa+1)}\int_0^h \psi(s)\,ds\int_0^\infty \xi c(I_0K_0-I_1K_1)\cos(\xi z)\sin(\xi s)\,d\xi\\&+\int_0^\infty \bar{A}(\xi)\left[\frac{1}{2}(\kappa-1)+\xi z\right]e^{-\xi z}J_0(\xi c)\,d\xi,\quad r=c,\quad 0\le z\le h\end{aligned} \tag{2.43}$$

$$\begin{aligned}2\mu u_r=&-\sqrt{\frac{\pi}{2}}\int_0^c \eta(\tau)\,d\tau\int_0^\infty \xi^{1/2}\left[\frac{1}{2}(\kappa+1)-\xi z\right]e^{-\xi z}J_1(\xi c)J_{3/2}(\xi\tau)\,d\xi\\&-\sqrt{\frac{\pi}{2}}\int_c^\infty \lambda(\tau)\,d\tau\int_0^\infty \xi^{1/2}\left[\frac{1}{2}(\kappa+1)-\xi z\right]e^{-\xi z}J_1(\xi c)J_{1/2}(\xi\tau)\,d\xi\\&+\frac{4c}{\pi(\kappa+1)}\int_0^h \phi(s)\,ds\int_0^\infty \xi c(I_0K_0-I_1K_1)\sin(\xi z)\cos(\xi s)\,d\xi\\&+\frac{4c}{\pi(\kappa+1)}\int_0^h \psi(s)\,ds\int_0^\infty [(\kappa+1)I_1K_1-\xi c(I_0K_1-I_1K_0)]\sin(\xi z)\sin(\xi s)\,d\xi\\&-\int_0^\infty \bar{A}(\xi)\left[\frac{1}{2}(\kappa+1)-\xi z\right]e^{-\xi z}J_1(\xi c)\,d\xi,\quad r=c,\quad 0\le z\le h.\end{aligned} \tag{2.44}$$

The rigidity of the cylindrical shell is assured by equating to zero the tangential derivatives of the displacements along the shell, $r=c, 0\le z\le h$, as described in eqns (2.5) and (2.6). By so doing, the tangential derivatives of vertical and radial displacements are calculated as given next (the superscript S will be used to refer to the shell solution):

$$\begin{aligned}(\kappa+1)\pi\mu\frac{\partial u_z^S}{\partial z}=&\frac{\kappa}{2}\int_0^h \phi(s)\left(\frac{1}{s-z}-\frac{1}{s+z}\right)ds\\&+2c\int_0^h \phi(s)\left\{\int_0^c S_1(s,\tau)[F_1(z,\tau)+G_1(z,\tau)]\,d\tau\right.\end{aligned}$$

$$+\int_c^\infty S_3(s,\tau)[F_2(z,\tau)+G_2(z,\tau)]\,d\tau+M_1(s,z)\Big\}\,ds$$
$$+2c\int_0^h \psi(s)\Big\{\int_0^c S_2(s,\tau)[F_1(z,\tau)+G_1(z,\tau)]\,d\tau$$
$$+\int_c^\infty S_4(s,\tau)[F_2(z,\tau)+G_2(z,\tau)]\,d\tau+M_2(s,z)\Big\}\,ds,\quad r=c,\,0\le z\le h \tag{2.45}$$

$$(\kappa+1)\pi\mu\frac{\partial u_r^S}{\partial z}=\frac{\kappa}{2}\int_0^h \psi(s)\left(\frac{1}{s-z}+\frac{1}{s+z}\right)ds$$
$$+2c\int_0^h \phi(s)\Big\{\int_0^c S_1(s,\tau)[F_3(z,\tau)+G_3(z,\tau)]\,d\tau$$
$$+\int_c^\infty S_3(s,\tau)[F_4(z,\tau)+G_4(z,\tau)]\,d\tau+M_3(s,z)\Big\}\,ds$$
$$+2c\int_0^h \psi(s)\Big\{\int_0^c S_2(s,\tau)[F_3(z,\tau)+G_3(z,\tau)]\,d\tau$$
$$+\int_c^\infty S_4(s,\tau)[F_4(z,\tau)+G_4(z,\tau)]\,d\tau+M_4(s,z)\Big\}\,ds,\quad r=c,\,0\le z\le h \tag{2.46}$$

where

$$M_1(s,z)=-\int_0^\infty\left\{\xi[(\kappa+1)I_0K_0-\xi c(I_0K_1-I_1K_0)]-\frac{\kappa}{2c}\right\}\sin(\xi z)\cos(\xi s)\,d\xi \tag{2.47}$$

$$M_2(s,z)=-\int_0^\infty \xi^2 c(I_0K_0-I_1K_1)\sin(\xi z)\sin(\xi s)\,d\xi \tag{2.48}$$

$$M_3(s,z)=\int_0^\infty \xi^2 c(I_0K_0-I_1K_1)\cos(\xi z)\cos(\xi s)\,d\xi \tag{2.49}$$

$$M_4(s,z)=\int_0^\infty\left\{\xi[(\kappa+1)I_1K_1-\xi c(I_0K_1-I_1K_0)]-\frac{\kappa}{2c}\right\}\cos(\xi z)\sin(\xi s)\,d\xi \tag{2.50}$$

$$F_1(z,\tau)=\sqrt{\frac{2}{\pi}}\tau^{-1/2}\int_0^\infty \xi^{3/2}\left[\frac{1}{2}(\kappa-3)-\xi z\right]e^{-\xi z}J_0(\xi c)J_{3/2}(\xi\tau)\,d\xi \tag{2.51}$$

$$F_2(z,\tau)=\sqrt{\frac{\pi}{2}}\tau^{1/2}\int_0^\infty \xi^{3/2}\left[\frac{1}{2}(\kappa-3)-\xi z\right]e^{-\xi z}J_0(\xi c)J_{1/2}(\xi\tau)\,d\xi \tag{2.52}$$

$$F_3(z,\tau)=\sqrt{\frac{2}{\pi}}\tau^{-1/2}\int_0^\infty \xi^{3/2}\left[\frac{1}{2}(\kappa+3)-\xi z\right]e^{-\xi z}J_1(\xi c)J_{3/2}(\xi\tau)\,d\xi \tag{2.53}$$

$$F_4(z,\tau)=\sqrt{\frac{\pi}{2}}\tau^{1/2}\int_0^\infty \xi^{3/2}\left[\frac{1}{2}(\kappa+3)-\xi z\right]e^{-\xi z}J_1(\xi c)J_{1/2}(\xi\tau)\,d\xi \tag{2.54}$$

$$G_1(z,\tau)=\frac{2}{\pi}\tau\int_c^\infty \frac{U_1(u,z)}{(u^2-\tau^2)^{3/2}}\,du \tag{2.55}$$

$$G_2(z,\tau)=\int_0^c \frac{u^2U_1(u,z)}{(\tau^2-u^2)^{3/2}}\,du \tag{2.56}$$

$$G_3(z,\tau)=\frac{2}{\pi}\tau\int_c^\infty \frac{U_2(u,z)}{(u^2-\tau^2)^{3/2}}\,du \tag{2.57}$$

$$G_4(z,\tau)=\int_0^c \frac{u^2U_2(u,z)}{(\tau^2-u^2)^{3/2}}du. \tag{2.58}$$

Here

$$U_1(u,z)=-\int_0^\infty \xi\left[\frac{1}{2}(\kappa-3)+\xi z\right]e^{-\xi z}J_0(\xi c)J_1(\xi u)\,d\xi \tag{2.59}$$

$$U_2(u, z) = \int_0^\infty \xi\left[\frac{1}{2}(\kappa + 3) - \xi z\right] e^{-\xi z} J_1(\xi c) J_1(\xi u)\, d\xi. \tag{2.60}$$

Thus, eqns (2.45) and (2.46), when used with eqns (2.5) and (2.6), provide the desired system of singular integral equations.

In order for eqns (2.45) and (2.46) to be suitable for numerical integration, the semi-infinite integrals, S_i, M_i, F_i, G_i $(i = 1, \ldots, 4)$ and U_i $(i = 1,2)$, contained in their kernels should be evaluated in closed form. The evaluation is indeed done for all of the integrals with the help of eqns (A5)–(A49) in the Appendix, except for the integrals G_i which have to be evaluated numerically.

The tangential derivatives of displacements along the plane $0 \le r \le c$, $z = h$, are also derived here. They will be used in the cylindrical rod problem in the next section.

$$\begin{aligned}(\kappa + 1)\pi\mu \frac{\partial u_z^S}{\partial r} = 2c \int_0^h \phi(s)\Big\{\int_0^c S_1(s, \tau)[R_1(r, \tau) + T_1(r, \tau)]\, d\tau + \int_c^\infty S_3(s, \tau)[R_2(r, \tau) + T_2(r, \tau)]\, d\tau \\ + N_1(s, r)\Big\}\, ds + 2c \int_0^h \psi(s)\Big\{\int_0^c S_2(s, \tau)[R_1(r, \tau) + T_1(r, \tau)]\, d\tau \\ + \int_c^\infty S_4(s, \tau)[R_2(r, \tau) + T_2(r, \tau)]\, d\tau + N_2(s, r)\Big\}\, ds, \quad 0 \le r \le c,\ z = h\end{aligned} \tag{2.61}$$

$$\begin{aligned}(\kappa + 1)\pi\mu \frac{\partial (r u_r^S)}{\partial r} = 2cr \int_0^h \phi(s)\Big\{\int_0^c S_1(s, \tau)[R_3(r, \tau) + T_3(r, \tau)]\, d\tau \\ + \int_c^\infty S_3(s, \tau)[R_4(r, \tau) + T_4(r, \tau)]\, d\tau + N_3(s, r)\Big\}\, ds \\ + 2cr \int_0^h \psi(s)\Big\{\int_0^c S_2(s, \tau)[R_3(r, \tau) + T_3(r, \tau)]\, d\tau \\ + \int_c^\infty S_4(s, \tau)[R_4(r, \tau) + T_4(r, \tau)]\, d\tau + N_4(s, r)\Big\}\, ds, \quad 0 \le r \le c,\ z = h\end{aligned} \tag{2.62}$$

where

$$N_1(s, r) = \int_0^\infty \xi\{[(\kappa + 1)K_0 - \xi c K_1] I_1(\xi r) + \xi r K_0 I_0(\xi r)\} \cos(\xi s) \cos(\xi h)\, d\xi \tag{2.63}$$

$$N_2(s, r) = \int_0^\infty \xi[\xi c K_0 I_1(\xi r) - \xi r K_1 I_0(\xi r)] \sin(\xi s) \cos(\xi h)\, d\xi \tag{2.64}$$

$$N_3(s, r) = \int_0^\infty \xi[(2K_0 - \xi c K_1) I_0(\xi r) + \xi r K_0 I_1(\xi r)] \cos(\xi s) \sin(\xi h)\, d\xi \tag{2.65}$$

$$N_4(s, r) = \int_0^\infty \xi\{[(\kappa - 1)K_1 + \xi c K_0] I_0(\xi r) - \xi r K_1 I_1(\xi r)\} \sin(\xi s) \sin(\xi h)\, d\xi \tag{2.66}$$

$$R_1(r, \tau) = -\sqrt{\frac{2}{\pi}}\, \tau^{-1/2} \int_0^\infty \xi^{3/2}\left[\frac{1}{2}(\kappa - 1) + \xi h\right] e^{-\xi h} J_1(\xi r) J_{3/2}(\xi \tau)\, d\xi \tag{2.67}$$

$$R_2(r, \tau) = -\sqrt{\frac{\pi}{2}}\, \tau^{1/2} \int_0^\infty \xi^{3/2}\left[\frac{1}{2}(\kappa - 1) + \xi h\right] e^{-\xi h} J_1(\xi r) J_{1/2}(\xi \tau)\, d\xi \tag{2.68}$$

$$R_3(r, \tau) = -\sqrt{\frac{2}{\pi}}\, \tau^{-1/2} \int_0^\infty \xi^{3/2}\left[\frac{1}{2}(\kappa + 1) - \xi h\right] e^{-\xi h} J_0(\xi r) J_{3/2}(\xi \tau)\, d\xi \tag{2.69}$$

$$R_4(r, \tau) = -\sqrt{\frac{\pi}{2}}\, \tau^{1/2} \int_0^\infty \xi^{3/2}\left[\frac{1}{2}(\kappa + 1) - \xi h\right] e^{-\xi h} J_0(\xi r) J_{1/2}(\xi \tau)\, d\xi \tag{2.70}$$

$$T_1(r, \tau) = \frac{2}{\pi}\, \tau \int_c^\infty \frac{U_3(u, r)}{(u^2 - \tau^2)^{3/2}}\, du \tag{2.71}$$

$$T_2(r, \tau) = \int_0^c \frac{u^2 U_3(u, r)}{(\tau^2 - u^2)^{3/2}}\, du \tag{2.72}$$

$$T_3(r,\tau)=\frac{2}{\pi}\tau\int_c^\infty\frac{U_4(u,r)}{(u^2-\tau^2)^{3/2}}\,du \tag{2.73}$$

$$T_4(r,\tau)=\int_0^c\frac{u^2U_4(u,r)}{(\tau^2-u^2)^{3/2}}\,du. \tag{2.74}$$

Here

$$U_3(u,r)=-\int_0^\infty\xi\left[\frac{1}{2}(\kappa-1)+\xi h\right]e^{-\xi h}J_1(\xi r)J_1(\xi u)\,d\xi \tag{2.75}$$

$$U_4(u,r)=-\int_0^\infty\xi\left[\frac{1}{2}(\kappa+1)-\xi h\right]e^{-\xi h}J_0(\xi r)J_1(\xi u)\,d\xi. \tag{2.76}$$

Similarly, semi-infinite integrals, N_i, R_i, and U_i $(i=1,\ldots,4)$ can be evaluated in closed form with the aid of eqns (A19)–(A49) in the Appendix. Integrals T_i $(i=1,\ldots,4)$ cannot be treated analytically and so have to be evaluated numerically.

Unknown functions, $\phi(s)$ and $\psi(s)$, can be determined from the solution of eqns (2.45) and (2.46) provided that the following subsidiary conditions are used:

$$2\pi c\int_0^h\phi(s)\,ds=-T \tag{2.77}$$

$$u_r(r=c,z=h/2)=0. \tag{2.78}$$

Equation (2.77) states that the resultant vertical load acting along the shell should equal $-T$, and eqn (2.78) ensures that the radial displacement of the shell is zero.

The order of singularity at the lower end of the shell is well known, but the singular behavior at the upper end must be obtained from the governing generalized singular integral equation by isolating the contributing parts from the entire equation.

If $\phi(s)$ and $\psi(s)$ are assumed to be the products of regular and singular parts in the following form:

$$\phi(s)=\bar{\phi}(s)s^{\eta_2-1} \tag{2.79}$$

$$\psi(s)=\bar{\psi}(s)s^{\eta_2-1} \tag{2.80}$$

where $0<\eta_2<1$, then, by taking asymptotic expansion of integrands when $\xi\to\infty$ and evaluating integrals after appropriate change of the orders of integration involved with the aid of eqns (A50)–(A54) in the Appendix, the correct upper end singular behavior can be obtained in the limiting case when $z\to0^+$ and $r\to c$:

$$\bar{\phi}(0)\pi z^{\eta_2-1}csc\eta_2\pi[2\kappa\cos\eta_2\pi+(\kappa^2+1)-4\eta_2^2]=0 \tag{2.81}$$

$$\bar{\psi}(0)\pi z^{\eta_2-1}csc\eta_2\pi[2\kappa\cos\eta_2\pi+(\kappa^2+1)-4\eta_2^2]=0. \tag{2.82}$$

It is obvious that both eqns (2.81) and (2.82) contain an identical eigenvalue equation. Equation (2.81) can be written after some rearrangement as follows:

$$\kappa^2\sin^2\frac{1}{2}\eta_2\pi=4(1-\nu)^2-\eta_2^2. \tag{2.83}$$

Equation (2.83) is in agreement with the eigenvalue equation determined by Williams [9] for a right-angle corner of an elastic plate in extension and therefore tends to confirm the present analysis.

When the value of $\nu=0.3$ is used for Poisson's ratio, η_2 is found equal to 0.71117.

The stress distribution along the cylindrical shell can be characterized by the load-transfer factor, $P(z)$, which is defined as:

$$P(z) = 2\pi c \int_z^h \phi(s)\,ds, \quad 0 \le z \le h. \tag{2.84}$$

3. RIGID ROD

The analysis herein considers a single rigid rod, partially embedded within the elastic half space. The same configuration as shown in Fig. 1 will be used. The rod is subjected to a resultant load, $-T$, directed along its axis. The rod is viewed as a cylindrical shell with its lower end closed by a rigid disk. A portion of the load will be carried by the base as well as the side of the rod. The surface of half space is stress free, and hence the following boundary conditions must be satisfied:

$$\tau_{zz} = 0, \quad 0 \le r < \infty, z = 0. \tag{3.1}$$
$$\tau_{zr} = 0, \tag{3.2}$$

The surface of rod which is in bonded contact with the half space is required to be rigid. Therefore, the tangential derivatives of both vertical and radial displacements are set equal to zero over the rod's surface, i.e.

$$\frac{\partial u_z}{\partial z} = 0, \quad r = c, \quad 0 \le z \le h \tag{3.3}$$

$$\frac{\partial u_r}{\partial z} = 0, \quad r = c, \quad 0 \le z \le h \tag{3.4}$$

$$\frac{\partial u_z}{\partial r} = 0, \quad 0 \le r \le c, \quad z = h \tag{3.5}$$

$$\frac{\partial (r u_r)}{\partial r} = 0, \quad 0 \le r \le c, \quad z = h. \tag{3.6}$$

The problems is formulated by the superposition of two solutions: (i) a shell solution developed in Section 2, and (ii) a plate solution to be given next. The plate solution is that for a rigid circular disk, $z = h$, $0 \le r \le c$, at the lower end of the shell. The function of the plate solution is to cause the material within the region, $0 \le z \le h$, $0 \le r \le c$, to move as a rigid body.

Plate solution

An infinite horizontal thin plate at a distance, h, below the half space surface subdivides it into two regions: region (L) which is a layer of uniform thickness, h, directly below the surface of half space, and region (H) which occupies the remaining portion of the half space. The displacement continuity conditions prescribed on the plate surface can be expressed as follows:

$$u_z^L = u_z^H, \quad 0 \le r < \infty, z = h. \tag{3.7}$$
$$u_r^L = u_r^H, \tag{3.8}$$

The displacements and stresses for regions (L) and (H) are expressed in terms of Hankel integral transforms for both regions.

Region (*L*): $(0 \le r < \infty, 0 \le z \le h)$

$$\begin{aligned} 2\mu u_z^L = \int_0^\infty & \{D_1(\xi)\cosh \xi(z-h) + D_2(\xi)\sinh \xi(z-h) \\ & + E_1(\xi)[\xi(z-h)\sinh \xi(z-h) - (3-4\nu)\cosh \xi(z-h)] \\ & + E_2(\xi)[\xi(z-h)\cosh \xi(z-h) - (3-4\nu)\sinh \xi(z-h)]\} J_0(\xi r)\,d\xi \end{aligned} \tag{3.9}$$

$$\begin{aligned} 2\mu u_r^L = -\int_0^\infty & \{D_1(\xi)\sinh \xi(z-h) + D_2(\xi)\cosh \xi(z-h) \\ & + \xi(z-h)\cdot[E_1(\xi)\cosh \xi(z-h) + E_2(\xi)\sinh \xi(z-h)]\} J_1(\xi r)\,d\xi \end{aligned} \tag{3.10}$$

$$\tau_{zz}^{L} = \int_0^\infty \xi\{D_1(\xi)\sinh\xi(z-h) + D_2(\xi)\cosh\xi(z-h) + E_1(\xi)\cdot[\xi(z-h)\cosh\xi(z-h) - 2(1-\nu)\sinh\xi(z-h)] + E_2(\xi)[\xi(z-h)\sinh\xi(z-h) - 2(1-\nu)\cosh\xi(z-h)]\}J_0(\xi r)\,d\xi \tag{3.11}$$

$$\tau_{zr}^{L} = -\int_0^\infty \xi\{D_1(\xi)\cosh\xi(z-h) + D_2(\xi)\sinh\xi(z-h) + E_1(\xi)\cdot[\xi(z-h)\sinh\xi(z-h) - (1-2\nu)\cosh\xi(z-h)] + E_2(\xi)[\xi(z-h)\cosh\xi(z-h) - (1-2\nu)\sinh\xi(z-h)]\}J_1(\xi r)\,d\xi. \tag{3.12}$$

Region (H): $(0 \le r < \infty,\ h \le z < \infty)$

$$2\mu u_z^H = \int_0^\infty \{-H_1(\xi) + [(3-4\nu) + \xi(z-h)]H_2(\xi)\}\,e^{-\xi(z-h)}J_0(\xi r)\,d\xi \tag{3.13}$$

$$2\mu u_r^H = \int_0^\infty [-H_1(\xi) + \xi(z-h)H_2(\xi)]\,e^{-\xi(z-h)}J_1(\xi r)\,d\xi \tag{3.14}$$

$$\tau_{zz}^H = \int_0^\infty \xi\{H_1(\xi) - [2(1-\nu) + \xi(z-h)]H_2(\xi)\}\,e^{-\xi(z-h)}J_0(\xi r)\,d\xi \tag{3.15}$$

$$\tau_{zr}^H = \int_0^\infty \xi\{H_1(\xi) - [(1-2\nu) + \xi(z-h)]H_2(\xi)\}\,e^{-\xi(z-h)}J_1(\xi r)\,d\xi. \tag{3.16}$$

After satisfying the boundary conditions in eqns (3.1) and (3.2) and the displacement continuity conditions in eqns (3.7) and (3.8), the stresses, τ_{zr}^H and τ_{zz}^H, can be expressed in terms of $E_1(\xi)$ and $E_2(\xi)$ in the following way:

$$\tau_{zr}^H = \frac{1}{4\kappa}\int_0^\infty \xi\{E_1(\xi)[\kappa(\kappa-1) + 2(\kappa+1)\xi h - e^{2\xi h} + \kappa\,e^{-2\xi h}] + E_2(\xi)[\kappa(\kappa+1) - 2(\kappa-1)\xi h + e^{2\xi h} + \kappa\,e^{-2\xi h}]\}J_1(\xi r)\,d\xi, \quad 0 \le r < \infty, \quad z = h \tag{3.17}$$

$$\tau_{zz}^H = \frac{1}{4\kappa}\int_0^\infty \xi\{E_1(\xi)[\kappa(\kappa+1) + 2(\kappa-1)\xi h + e^{2\xi h} + \kappa\,e^{-2\xi h}] + E_2(\xi)[\kappa(\kappa-1) - 2(\kappa+1)\xi h - e^{2\xi h} + \kappa\,e^{-2\xi h}]\}J_0(\xi r)\,d\xi, \quad 0 \le r < \infty, \quad z = h. \tag{3.18}$$

If the jumps in stresses, $\chi(r)$ and $\omega(r)$, across the plate surface are defined in the following manner:

$$\begin{aligned} \chi(r) &= \tau_{zr}^L - \tau_{zr}^H, \\ \omega(r) &= \tau_{zz}^L - \tau_{zz}^H, \end{aligned} \qquad 0 \le r \le c, \quad z = h \tag{3.19}$$

then through the application of Hankel transforms, the displacements in the layer region (L) can be expressed in terms of $\chi(r)$ and $\omega(r)$ as follows:

$$2\mu u_z^L = \frac{1}{\kappa+1}\int_0^c t\omega(t)\,dt\int_0^\infty \left\{[\kappa + \xi(h-z)]\,e^{-\xi(h-z)} + \left[\frac{1}{2}(\kappa^2+1) + \kappa\xi(h+z) + 2\xi^2 hz\right]e^{-\xi(h+z)}\right\}J_0(\xi t)J_0(\xi r)\,d\xi + \frac{1}{\kappa+1}\int_0^c t\chi(t)\,dt\int_0^\infty \left\{\xi(h-z)\,e^{-\xi(h-z)} + \left[-\frac{1}{2}(\kappa^2-1) + \kappa\xi(h-z) + 2\xi^2 hz\right]e^{-\xi(h+z)}\right\}J_1(\xi t)J_0(\xi r)\,d\xi, \quad 0 \le r \le c, \quad 0 \le z \le h \tag{3.20}$$

$$2\mu u_r^L = \frac{1}{\kappa+1}\int_0^c t\omega(t)\,dt\int_0^\infty \left\{-\xi(h-z)\,e^{-\xi(h-z)} - \left[\frac{1}{2}(\kappa^2-1) + \kappa\xi(h-z) - 2\xi^2 hz\right]e^{-\xi(h+z)}\right\}J_0(\xi t)J_1(\xi r)\,d\xi + \frac{1}{\kappa+1}\int_0^c t\chi(t)\,dt\int_0^\infty \left\{[\kappa - \xi(h-z)]\,e^{-\xi(h-z)}\right.$$

$$+\left[\frac{1}{2}(\kappa^2+1)-\kappa\xi(h+z)+2\xi^2hz\right]e^{-\xi(h+z)}\Big\}J_1(\xi t)J_1(\xi r)\,d\xi,\quad 0\le r\le c,\ 0\le z\le h. \tag{3.21}$$

The tangential derivatives of vertical and radial displacements along the cylindrical surface of the rod due to the plate solution are found to have the following expressions (the superscript P will be used to refer to the plate solution):

$$\begin{aligned}(\kappa+1)\pi\mu\frac{\partial u_z^P}{\partial z}=&\frac{\pi}{2}\int_0^c t\omega(t)\,dt\int_0^\infty \xi\Big\{[(\kappa-1)+\xi(h-z)]e^{-\xi(h-z)}\\&-\left[\frac{1}{2}(\kappa-1)^2+\kappa\xi(h+z)-2\xi h(1-\xi z)\right]e^{-\xi(h+z)}\Big\}J_0(\xi t)J_0(\xi c)\,d\xi\\&+\frac{\pi}{2}\int_0^c t\chi(t)\,dt\int_0^\infty \xi\Big\{[-1+\xi(h-z)]e^{-\xi(h-z)}\\&+\left[\frac{1}{2}(\kappa^2-2\kappa-1)-\kappa\xi(h-z)+2\xi h(1-\xi z)\right]e^{-\xi(h+z)}\Big\}J_1(\xi t)J_0(\xi c)\,d\xi,\quad r=c,\\&\qquad 0\le z\le h\end{aligned} \tag{3.22}$$

$$\begin{aligned}(\kappa+1)\pi\mu\frac{\partial u_r^P}{\partial z}=&\frac{\pi}{2}\int_0^c t\omega(t)\,dt\int_0^\infty \xi\Big\{[1-\xi(h-z)]e^{-\xi(h-z)}\\&+\left[\frac{1}{2}(\kappa^2+2\kappa-1)+\kappa\xi(h-z)+2\xi h(1-\xi z)\right]e^{-\xi(h+z)}\Big\}J_0(\xi t)J_1(\xi c)\,d\xi\\&+\frac{\pi}{2}\int_0^c t\chi(t)\,dt\int_0^\infty \xi\Big\{[(\kappa+1)-\xi(h-z)]e^{-\xi(h-z)}\\&-\left[\frac{1}{2}(\kappa+1)^2-\kappa\xi(h+z)-2\xi h(1-\xi z)\right]e^{-\xi(h+z)}\Big\}J_1(\xi t)J_1(\xi c)\,d\xi,\quad r=c,\\&\qquad 0\le z\le h\end{aligned} \tag{3.23}$$

$$\begin{aligned}(\kappa+1)\pi\mu\frac{\partial u_z^P}{\partial r}=&\frac{1}{2}\kappa\int_0^c \omega(t)\left(\frac{1}{t-r}-\frac{1}{t+r}\right)g_1(t,r)\,dt\\&-\pi\int_0^c t\omega(t)\,dt\int_0^\infty \xi\left[\frac{1}{4}(\kappa^2+1)+\kappa\xi h+\xi^2h^2\right]e^{-2\xi h}J_0(\xi t)J_1(\xi r)\,d\xi\\&-\pi\int_0^c t\chi(t)\,dt\int_0^\infty \xi\left[-\frac{1}{4}(\kappa^2-1)+\xi^2h^2\right]e^{-2\xi h}J_1(\xi t)J_1(\xi r)\,d\xi,\quad 0\le r\le c,\quad z=h\end{aligned} \tag{3.24}$$

$$\begin{aligned}(\kappa+1)\pi\mu\frac{\partial(ru_r^P)}{\partial r}=&\frac{1}{2}\kappa r\int_0^c \chi(t)\left(\frac{1}{t-r}+\frac{1}{t+r}\right)g_2(t,r)\,dt\\&+\pi r\int_0^c t\omega(t)\,dt\int_0^\infty \xi\left[-\frac{1}{4}(\kappa^2-1)+\xi^2h^2\right]e^{-2\xi h}J_0(\xi t)J_0(\xi r)\,d\xi\\&+\pi r\int_0^c t\chi(t)\,dt\int_0^\infty \xi\left[\frac{1}{4}(\kappa^2+1)-\kappa\xi h+\xi^2h^2\right]e^{-2\xi h}J_1(\xi t)J_0(\xi r)\,d\xi,\quad 0\le r\le c,\\&\qquad z=h\end{aligned} \tag{3.25}$$

where

$$g_1(t,r)=\begin{cases}\dfrac{t}{r}E\left(\dfrac{t}{r}\right), & t<r\\[2ex] \dfrac{t^2}{r^2}E\left(\dfrac{r}{t}\right)-\dfrac{t^2-r^2}{r^2}K\left(\dfrac{r}{t}\right), & t>r\end{cases} \tag{3.26}$$

$$g_2(t,r)=\begin{cases}\dfrac{r}{t}E\left(\dfrac{t}{r}\right)+\dfrac{t^2-r^2}{tr}K\left(\dfrac{t}{r}\right), & t<r\\[2ex] E\left(\dfrac{r}{t}\right), & t>r\end{cases} \tag{3.27}$$

Here K and E are complete elliptic integrals of the first and the second kind, respectively (Oberhettinger[10]). The kernels in eqns (3.22)–(3.25) are semi-infinite integrals which can be evaluated in closed form to facilitate numerical programming with the help of eqns (A37)–(A49) in the Appendix.

The desired solution of the rod can be obtained when the shell solution in Section 2 is linearly superimposed with the plate solution. When eqns (2.45), (2.46), (2.61) and (2.62) for the shell solution and eqns (3.22)–(3.25) for the plate solution are superimposed appropriately after satisfying eqns (3.3)–(3.6) to ensure the rigidity of the rod surface, a system of four coupled singular integral equations is obtained as given next:

$$\frac{\partial u_z}{\partial z} = \frac{\partial u_z^S}{\partial z} + \frac{\partial u_z^P}{\partial z} = 0, \qquad r = c, \quad 0 \le z \le h \tag{3.28}$$

$$\frac{\partial u_r}{\partial z} = \frac{\partial u_r^S}{\partial z} + \frac{\partial u_r^P}{\partial z} = 0, \qquad r = c, \quad 0 \le z \le h \tag{3.29}$$

$$\frac{\partial u_z}{\partial r} = \frac{\partial u_z^S}{\partial r} + \frac{\partial u_z^P}{\partial r} = 0, \qquad 0 \le r \le c, \quad z = h \tag{3.30}$$

$$\frac{\partial (ru_r)}{\partial r} = \frac{\partial (ru_r^S)}{\partial r} + \frac{\partial (ru_r^P)}{\partial r} = 0, \qquad 0 \le r \le c, \quad z = h. \tag{3.31}$$

The unknown functions in the form of stress jumps, $\phi(z)$, $\psi(z)$, $\chi(r)$ and $\omega(r)$, can be determined from the solution of this system of equations provided that the following subsidiary conditions are used:

$$2\pi c \int_0^h \phi(s)\,\mathrm{d}s + 2\pi \int_0^c t\omega(t)\,\mathrm{d}t = -T \tag{3.32}$$

$$u_z\left(r = c, z = \frac{1}{2}h\right) - u_z(r = 0, z = h) = 0 \tag{3.33}$$

$$u_r(r = c, z = h) = 0 \tag{3.34}$$

$$\chi(0) = 0. \tag{3.35}$$

In eqn (3.32), the first term designates the total load, P_s, acting on the side of rod while the second term is for the total load, P_b, acting on the base of rod. Therefore eqn (3.32) is a statement of overall equilibrium by requiring the resultant vertical load acting on the rod equal to $-T$, or equivalently,

$$P_s + P_b = -T. \tag{3.36}$$

Equation (3.33) ensures that the side and the base of rod will undergo vertical displacement as a rigid body. Zero radial displacement is a mechanical constraint imposed on the rod by eqn (3.34). Equation (3.35) is necessary for the purpose of the numerical solution technique used, and its involvement will be explained later in the next section.

The plate solution does not contribute to the singular behavior when investigating the upper end of the rod, and therefore the upper end of the rod has the same singular behavior as that of the cylindrical shell. The singular behavior at the lower end of rod can be derived from the governing generalized singular integral equations by following similar analytical evaluation procedures.

If the stress jumps are assumed to be in the following form of the products of regular and singular parts:

$$\phi(s) = \hat{\phi}(s)(h - s)^{\eta_1 - 1} \tag{3.37}$$

$$\psi(s) = \hat{\psi}(s)(h - s)^{\eta_1 - 1} \tag{3.38}$$

$$\chi(t) = \hat{\chi}(t)(c - t)^{\eta_1 - 1} \tag{3.39}$$

$$\omega(t) = \hat{\omega}(t)(c - t)^{\eta_1 - 1} \tag{3.40}$$

where $0 < \eta_1 < 1$, then the system of four coupled singular integral equations will yield the following four equations for the corners after evaluating the involved integrals in the limiting case when $z \to h$ and $r \to c$:

$$\kappa \cos \eta_1 \pi \hat{\phi}(h) + (\kappa - \eta_1) \cos \frac{1}{2} \eta_1 \pi \hat{\omega}(c) + \eta_1 \sin \frac{1}{2} \eta_1 \pi \hat{\chi}(c) = 0 \tag{3.41}$$

$$\kappa \cos \eta_1 \pi \hat{\psi}(h) + \eta_1 \sin \frac{1}{2} \eta_1 \pi \hat{\omega}(c) + (\kappa + \eta_1) \cos \frac{1}{2} \eta_1 \pi \hat{\chi}(c) = 0 \tag{3.42}$$

$$(\kappa + \eta_1) \cos \frac{1}{2} \eta_1 \pi \hat{\phi}(h) + \eta_1 \sin \frac{1}{2} \eta_1 \pi \hat{\psi}(h) + \kappa \cos \eta_1 \pi \hat{\omega}(c) = 0 \tag{3.43}$$

$$\eta_1 \sin \frac{1}{2} \eta_1 \pi \hat{\phi}(h) + (\kappa - \eta_1) \cos \frac{1}{2} \eta_1 \pi \hat{\psi}(h) + \kappa \cos \eta_1 \pi \hat{\chi}(c) = 0. \tag{3.44}$$

The above equations for the corners can be shown to lead to the following eigenvalue equation:

$$\left(\kappa^2 \sin^2 \frac{3}{2} \eta_1 \pi - \eta_1^2\right)\left(\kappa^2 \sin^2 \frac{1}{2} \eta_1 \pi - \eta_1^2\right) = 0. \tag{3.45}$$

The correct lower end singular behavior can be obtained when η_1 is determined from

$$\kappa^2 \sin^2 \frac{3}{2} \eta_1 \pi - \eta_1^2 = 0. \tag{3.46}$$

There are two roots of η_1 which can be obtained from the foregoing equation. The one which will yield stronger singularity at the lower end is chosen for numerical computation. In so doing, η_1 is found equal to 0.59516 for $\nu = 0.3$.

Equation (3.46) has the identical form as the eigenvalue equation established by Williams [9] for a right-angle corner of an elastic plate in extension and hence tends to confirm the present analysis.

The load diffusion through the rod can be characterized by the load-transfer factor, $P(z)$, which is defined as:

$$P(z) = P_b + 2\pi c \int_z^h \phi(s)\, ds, \qquad 0 \le z \le h. \tag{3.47}$$

4. NUMERICAL ANALYSIS AND DISCUSSION OF RESULTS

In order to facilitate numerical integration, the system of coupled singular integral equations is normalized and appropriate singularities are given to the stress jumps at the end points. This is done by introducing the following changes of variables and definitions:

$$\gamma = c/h \tag{4.1}$$

$$s = \frac{1}{2} h(1 + s_0); \qquad z = \frac{1}{2} h(1 + z_0) \tag{4.2a,b}$$

$$t = ct_0; \qquad r = cr_0 \tag{4.3a,b}$$

$$\tau = c\tau_0; \qquad \xi = \xi_0/h \tag{4.4a,b}$$

and

$$\phi(s) = \Phi(s_0) \frac{T}{\pi c h} (1 - s_0)^{\eta_1 - 1} (1 + s_0)^{\eta_2 - 1} \tag{4.5}$$

$$\psi(s) = \Psi(s_0) \frac{T}{\pi c h} (1 - s_0)^{\eta_1 - 1} (1 + s_0)^{\eta_2 - 1} \tag{4.6}$$

$$\chi(t) = \mathrm{X}(t_0)\frac{T}{2\pi c^2}(1-t_0^2)^{\eta_1-1} \tag{4.7}$$

$$\omega(t) = \Omega(t_0)\frac{T}{2\pi c^2}(1-t_0^2)^{\eta_1-1} \tag{4.8}$$

It is noted that there are only two unknown stress jumps, $\phi(s)$ and $\psi(s)$, in the cylindrical shell problem where η_1 is equal to 0.5.

The numerical solution technique is based on the Gauss–Jacobi integration scheme described by Erdogan *et al.*[8]. This scheme is applicable to the rod problem after an extension of the definition of the stress jumps, $\chi(t)$ and $\omega(t)$, into the negative domain has been adapted. A similar technique of this kind has been used by Gupta and Erdogan[11]. A review on the definition of stress jumps in eqn (3.19) suggests that $\omega(t)$ should be even cotinuation and $\chi(t)$ ought to be odd continuation. This brings about the restriction on $\chi(t)$ described in eqn (3.35) as a subsidiary condition to be satisfied for the numerical solution of the system of coupled singular integral equations.

Gauss–Jacobi scheme provides integration points, s_i and t_j, and collocation points, z_i and r_j, defined as the roots of Jacobi-polynomials as follows:

$$P_n^{(\eta_1-1,\,\eta_2-1)}(s_i) = 0; \qquad P_{n-1}^{(\eta_1,\eta_2)}(z_i) = 0 \tag{4.9}$$

$$P_n^{(\eta_1-1,\,\eta_2-1)}(t_j) = 0; \qquad P_{n-1}^{(\eta_1,\eta_2)}(r_j) = 0. \tag{4.10}$$

The corresponding weights can also be obtained from the Gauss–Jacobi integration formula.

It is noted that the numerical scheme adapted in this paper works accurately for the shell problem, but for the rod problem it fails to properly treat the singular behavior at its lower end, and thus possible inaccuracy of the end-point values for stresses may result. Nonetheless, the accuracy of the global mechanical behavior of the rod which is of interest in this paper should not suffer excessively from this drawback. The accuracy of the numerical solution will be discussed at length later in this section.

For the cylindrical shell problem, a set of $2n \times 2n$ simultaneous algebraic equations in $2n$ unknowns, $\Phi(s_i)$ and $\Psi(s_i)$, is required in order to obtain numerical solutions. The system of two coupled singular integral equations provides $2n-2$ equations, while the remaining two equations must be supplied by the two subsidiary conditions described in eqns (2.77) and (2.78).

Similarly, a set of $4n \times 4n$ simultaneous algebraic equations in $4n$ unknowns, $\Phi(s_i)$, $\Psi(s_i)$, $\Omega(t_j)$ and $\mathrm{X}(t_j)$, is required in order to obtain numerical solutions for the rod problem. The system of four coupled singular integral equations provides $4n-4$ equations, and the four subsidiary conditions described in eqns (3.32)–(3.35) supply the other four equations.

The convergence of the integration scheme used for the cylindrical shell problem is measured in terms of the total lateral load, Q_s, transmitted along the shell. By definition, Q_s is given by

$$\frac{Q_s}{T} = \int_{-1}^{1} \Psi(s_0)(1-s_0)^{\eta_1-1}(1+s_0)^{\eta_2-1}\,\mathrm{d}s_0. \tag{4.11}$$

The total vertical load carried by the side of rod, P_s, is used as a measure of the convergence of the integration scheme used for the rod problem. By definition, P_s is given by

$$\frac{P_s}{T} = \int_{-1}^{1} \Phi(s_0)(1-s_0)^{\eta_1-1}(1+s_0)^{\eta_2-1}\,\mathrm{d}s_0. \tag{4.12}$$

The behavior of the convergence of the collocation scheme for various values of γ is shown in Table 1 for the shell problem and in Table 2 for the rod problem. It can be seen that in both tables the rate of convergence slows down rapidly with decreasing values of γ, i.e. as the shell and the rod become more slender.

The distributions of shear stresses along the side of shell and rod are shown in Figs. 2 and 3,

Table 1. Convergence of the algorithm for the cylindrical shell using different aspect ratios, $\gamma = c/h$. The reported values represent Q_s/T

Number of integration points	γ			
	2.0	1.0	0.5	0.2
8	−0.36592			
16	−0.36463	−0.60329		
24		−0.59873		
32			−1.07908	
40			−1.07263	−2.92588
48				−2.90221

Table 2. Convergence of the algorithm for the cylindrical rod using different aspect ratios, $\gamma = c/h$. The reported values represent P_s/T

Number of integration points	γ			
	2.0	1.0	0.5	0.2
8	0.31182			
16	0.30857	0.50713		
24		0.50376		
32			0.63806	
40			0.63128	
50				0.73814
60				0.72986

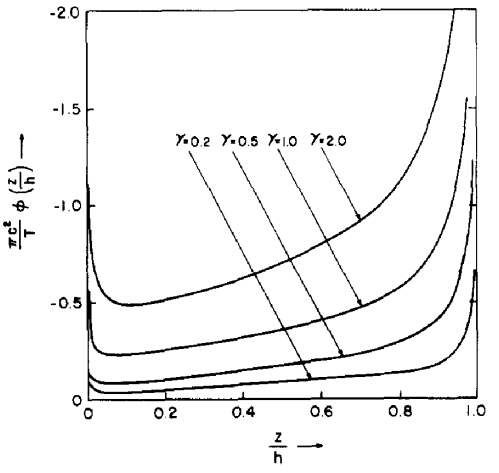

Fig. 2.

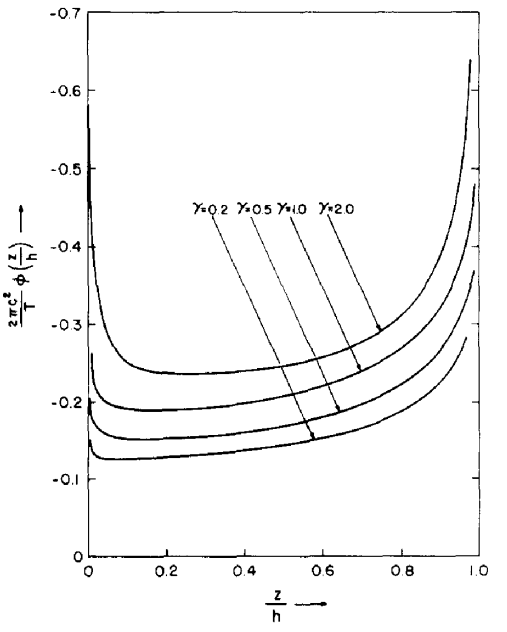

Fig. 3.

Fig. 2. Distribution of shear stresses along the side of the shell.

Fig. 3. Distribution of shear stresses along the side of the rod.

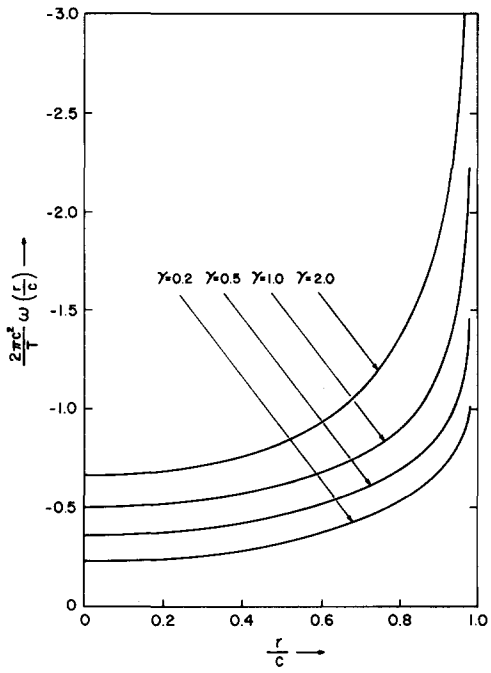

Fig. 4.

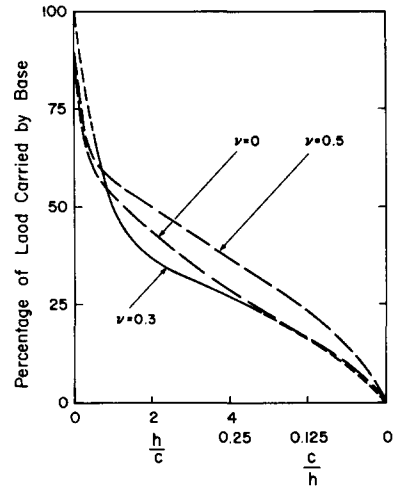

Fig. 5.

Fig. 4. Distribution of normal stresses on the base of the rod.

Fig. 5. Variation of the base load of the rod with its aspect ratio; dashed curves are the results from Poulos and Davis[1].

respectively. There is a local concentration of shear stress built up around both upper and lower ends of shell and rod. A comparison with the shear stress distributions obtained by Poulos and Davis[1] will show that the distributions presented in Figs. 2 and 3 are considerably smoother. The reason for this appearance may be the inclusion of normal stress along the side of shell and rod and shear stress on the base of rod, which are not included in their analysis. Figure 4 shows the distribution of normal stresses on the base of rod. There is also a local concentration of normal stress around the edge of rod.

The percentage of vertical load carried by the base of rod is plotted in Fig. 5 vs the aspect ratio. A comparison is made in the same figure with the results derived by Poulos and Davis[1]. Both results seem to follow the same trend of variation, even though their magnitudes are not particularly close. Such a discrepancy is within expectation because of the approximate method and assumptions employed by Poulos and Davis to obtain their results.

The vertical displacements for the shell and the rod on the surface of half space, $z = 0$, are shown in Figs. 6 and 7, respectively. It can be seen that the maximum displacement within the shell, $|u_z(0,0) - u_z(c,0)|$, is tending to become smaller with respect to a point two diameters away as γ becomes smaller. This suggests that for $\gamma \leq 0.2$ the shell solution might give a good approximation to a rigid rod. Under the same loading conditions, the shell is displaced more than the rod. This implies that the rod is mechanically stiffer than the shell. The elastic material at any point on the top surface of the rod has almost the same vertical displacement as at its rim; hence the elastic material within the rod undergoes a rigid body displacement when the superposition of solutions is taken into account.† This result can be looked upon as a check for the global accuracy of the numerical solutions, provided c/h is sufficiently small.

The load diffusion characteristics of the shell and the rod are determined by eqns (2.84) and

†Since the material "interior" to the rod undergoes a rigid body displacement, the "stress jumps" are, in reality the actual stresses on the rod's surface.

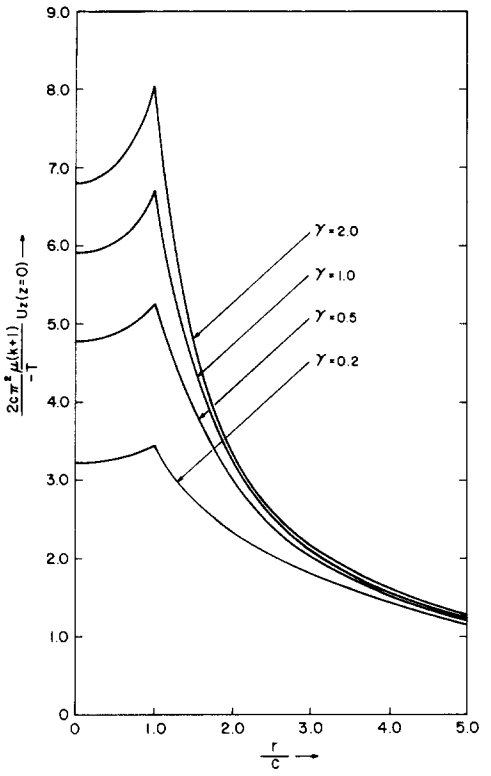

Fig. 6.

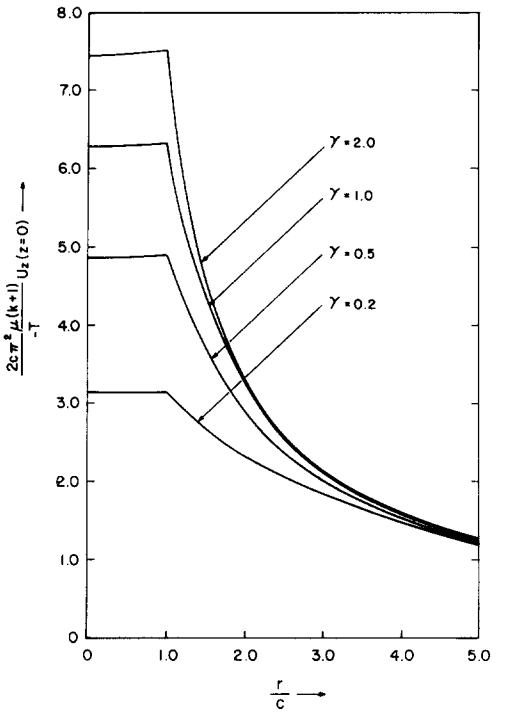

Fig. 7.

Fig. 6. Vertical displacements of the shell on the surface of half space.

Fig. 7. Vertical displacements of the rod on the surface of half space.

(3.47), respectively. The load-transfer curves for both the shell and the rod are plotted in Fig. 8 for various values of γ. The portion of the resultant load carried by the base of rod decreases as the rod becomes more slender so that the load-transfer curves for rod fall lower with decreasing value of γ. The reverse trend happens with the load-transfer curves for the shell. The two sets of curves are therefore approaching each other as the length increases with respect to the radius. One expects that when the aspect ratio is sufficiently small, the difference between the shell and the rod solutions becomes negligible.

For rather slender shells and rods the present results should compare with those of Muki and Sternberg[3]. In Fig. 9, the present load-transfer curves for $\gamma = 0.2$ are compared with their result for $\gamma = 0.2$ and $\nu = 0.25$. Their curve shown in Fig. 9 is obtained by using the technique of polynomial least squares curve fit to extrapolate the results of Ref.[3] for the case $\delta \to \infty$, which corresponds to a rigid rod. The method of extrapolation is indicated in Fig. 10. It can be seen from Fig. 9 that their curve falls mostly between the curves for the shell and the rod. Coincidentally, the extrapolated curve of Muki and Sternberg has almost the same percentage of resultant load carried by the base of rigid rod as that in this analysis; however, this agreement should not be considered to hint anything more than what is shown in Fig. 9, since there is a considerable amount of uncertainty involved in obtaining the extrapolated curve; a fully quantitative consideration of the position of the load-transfer curves obtained from the present analysis relative to the extrapolated curve might be misleading. One should bear this in mind especially when considering the comparison of solutions given by Muki and Sternberg in Ref.[4] where it shows that their exact solution tends to fall below the solution obtained by their approximate scheme.

It should be noted that for the rod problem the solution technique may not yield the correct

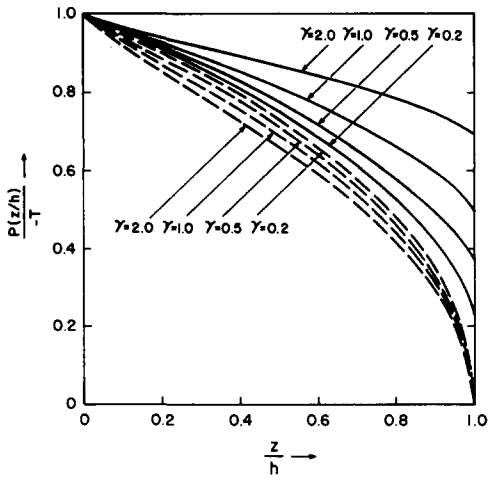

Fig. 8.

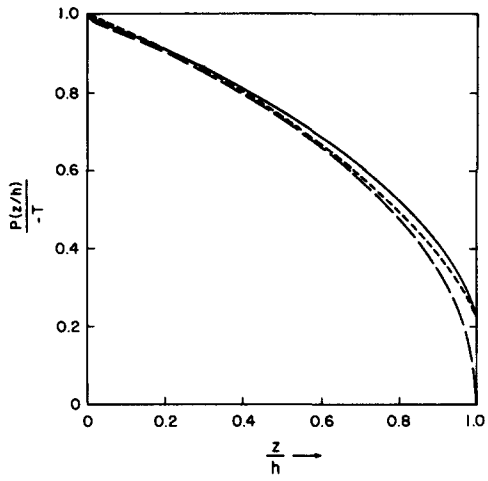

Fig. 9.

Fig. 8. Load-transfer characteristics of the shell and the rod; dashed curves are for the shell and solid curves are for the rod.

Fig. 9. Comparison of load-transfer curves for $\gamma = 0.2$; solid curve is for the rod, large dashed curve is for the shell, and small dashed curve is for the extrapolated results from Muki and Sternberg for $\nu = 0.25$.

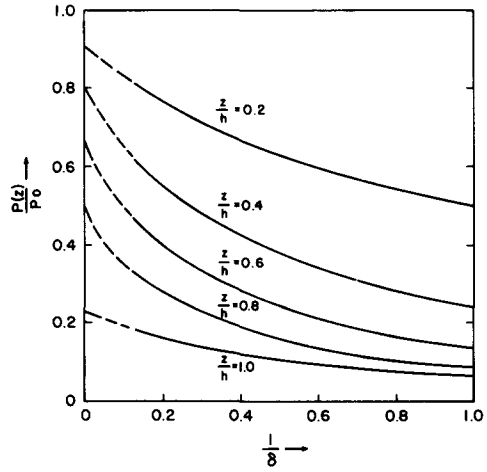

Fig. 10. Extrapolation of the load-transfer results from Muki and Sternberg[3]; $\delta \to \infty$ corresponds to a rigid rod.

end-point values for the stresses using the collocation scheme given in this paper, as suggested by Theocaris and Ioakimidis[12], and points very close to the end (c, h) are probably in error. There are two reasons accounting for this fact: (1) the collocation scheme of Gupta and Erdogan[11] does not necessarily give good accuracy at the end-points for generalized singular integral equations, and (2) the occurrence of two negative roots at the lower end may not be properly taken care of by the present scheme. Nevertheless, the global mechanical behavior of the shell and the rod should be given to within the accuracy demonstrated by the degree of convergence shown in Tables 1 and 2.

Acknowledgement—This work was supported in part by the U.S. National Science Foundation, Grant ENG-77-22155.

REFERENCES

1. H. G. Poulos and E. H. Davis, The settlement behavior of single axially loaded incompressible piles and piers. *Geotechnique* **18**, 351–371 (1968).
2. R. D. Mindlin, Force at a point in the interior of a semi-infinite solid. *Physics* **7**, 195–202 (1936).
3. R. Muki and E. Sternberg, Elastostatic load-transfer to a half-space from a partially embedded axially loaded rod. *Int. J. Solids Structures* **6**, 69–90 (1970).
4. R. Muki and E. Sternberg, On the diffusion of an axial load from an infinite cylindrical bar embedded in an elastic medium. *Int. J. Solids Structures* **5**, 587–605 (1969).
5. S. Suriyamongkal, P. Karasudhi and S. L. Lee, Axially Loaded Rigid Cylindrical Body Embedded in an Elastic Half-Space. *13th Midwestern Mechanics Conference*, University of Pittsburgh, 333–347 (1973).
6. J. W. Harding and I. N. Sneddon, The elastic stresses produced by the indentation of the plane surface of a semi-infinite elastic solid by a rigid punch. *Proc. Cambridge Phil. Soc.* **41**, 16–26 (1945).
7. G. K. Haritos and L. M. Keer, Stress analysis for an elastic half space containing an embedded rigid block. *Int. J. Solids Structures*, in press.
8. F. Erdogan, G. D. Gupta and T. S. Cook, Numerical Solution of Singular Integral Equations. In: *Methods of Analysis and Solutions of Crack Problems* 368–425. Noordhoff, Leyden (1973).
9. M. L. Williams, Stress singularities resulting from various boundary conditions in angular corners of plates in extension. *J. Appl. Mech.* **19**, *Trans. ASME* **74**, 526–528 (1952).
10. F. Oberhettinger, *Tables of Bessel Transforms*. Springer-Verlag, New York (1972).
11. G. D. Gupta and F. Erdogan, The problem of edge cracks in an infinite strip. *J. Appl. Mech.* **41**, *Trans. ASME* **E96**, 1001–1006 (1974).
12. P. S. Theocaris and N. I. Ioakimidis, Stress intensity factors at the tips of an antiplane shear crack terminating at a bimaterial interface. *Int. J. Fract.* **13**, 549–552 (1977).
13. R. A. Westmann, Asymmetric mixed boundary-value problems of the elastic half-space. *J. Appl. Mech.* **32**, *Trans. ASME* **E87**, 411–416 (1965).
14. I. N. Sneddon, *Fourier Transforms*, McGraw-Hill, New York (1951).
15. A. Erdelyi (Ed), *Tables of Integral Transforms*, Vols. 1 and 2. McGraw-Hill, New York (1954).
16. G. Eason, B. Noble and I. N. Sneddon, On certain integrals of Lipschitz–Hankel type involving products of Bessel functions. *Phil. Trans. R. Soc. Lond.* **A247**, (935), 529–551 (1955).

APPENDIX

The following notations are used in integral identities in eqns (A5)–(A28):

$$P_{vc} = c^2 + v^2 - t^2 \tag{A1}$$

$$Q_{vc} = (P_{vc}^2 + 4v^2t^2)^{1/2} \tag{A2}$$

$$M_{vc} = (Q_{vc} - P_{vc})^{1/2} \tag{A3}$$

$$N_{vc} = (Q_{vc} + P_{vc})^{1/2} \tag{A4}$$

where v can be either z or s.

The identities given below in eqns (A5)–(A28) are derived either directly or indirectly from Westmann[13] and Sneddon[14] with the help of Erdelyi[15].

$$\int_0^\infty \xi^{3/2} e^{-\xi z} J_0(\xi c) J_{3/2}(\xi t)\, d\xi = \frac{1}{\sqrt{\pi} t^{3/2} Q_{zc}^3}\{-zt(c^2+z^2+t^2)N_{zc} + [(c^2+z^2)^2 + t^2(2t^2+3z^2-3c^2)]M_{zc}\} \tag{A5}$$

$$\begin{aligned}\int_0^\infty \xi^{5/2} e^{-\xi z} J_0(\xi c) J_{3/2}(\xi t)\, d\xi = {} & \frac{1}{\sqrt{\pi} t^{3/2} Q_{zc}^5}\{-2tN_{zc}[(z^2-t^2)(c^2+z^2+t^2)^2 + 4c^2t^2(2z^2+t^2)] \\ & + zM_{zc}[(c^2+z^2+t^2)^3 + 4t^2(z^2+t^2)^2 - 4c^2t^2(3c^2+2z^2)]\} \\ & - \frac{1}{2\sqrt{\pi} t^{3/2} Q_{zc}^4}\{tN_{zc}(-c^2+z^2+t^2)(c^2+z^2+t^2-Q_{zc}) - zM_{zc}(c^2+z^2+t^2)(c^2+z^2+t^2+Q_{zc})\}\end{aligned} \tag{A6}$$

$$\int_0^\infty \xi^{3/2} e^{-\xi z} J_0(\xi c) J_{1/2}(\xi t)\, d\xi = \frac{1}{\sqrt{\pi} t^{1/2} Q_{zc}^3}[t(-c^2+z^2+t^2)N_{zc} + z(c^2+z^2+t^2)M_{zc}] \tag{A7}$$

$$\begin{aligned}\int_0^\infty \xi^{5/2} e^{-\xi z} J_0(\xi c) J_{1/2}(\xi t)\, d\xi = {} & -\frac{1}{\sqrt{\pi} t^{1/2} Q_{zc}^5}\{4ztN_{zc}[(c^2+z^2+t^2)(2c^2-z^2-t^2) - 2c^2t^2] \\ & + M_{zc}[(c^2-3z^2+t^2)(c^2+z^2+t^2)^2 - 4c^2t^2(c^2+3z^2+t^2)]\} \\ & - \frac{1}{2\sqrt{\pi} t^{3/2} Q_{zc}^4}\{zN_{zc}(c^2+z^2+t^2)(c^2+z^2+t^2-Q_{zc}) + tM_{zc}(-c^2+z^2+t^2)(c^2+z^2+Q_{zc})\}\end{aligned} \tag{A8}$$

$$\int_0^\infty \xi^{3/2} e^{-\xi z} J_1(\xi c) J_{3/2}(\xi t)\, d\xi = \frac{1}{\sqrt{\pi} c t^{3/2} Q_{zc}^3}\{tN_{zc}[(c^2+z^2+t^2)(z^2+t^2) - 2c^2t^2] - zM_{zc}[(c^2+z^2+t^2)^2 - 6c^2t^2]\} \tag{A9}$$

$$\begin{aligned}\int_0^\infty \xi^{5/2} e^{-\xi z} J_1(\xi c) J_{3/2}(\xi t)\, d\xi = {} & \frac{c}{\sqrt{\pi} t^{3/2} Q_{zc}^5}\{-2ztN_{zc}[(c^2+z^2+t^2)(c^2+z^2-5t^2) + 8c^2t^2] \\ & + M_{zc}[P_{zc}Q_{zc}^2 - 2t^2(c^2+z^2+t^2)(c^2-5z^2+t^2) + 8c^2t^4]\} \\ & - \frac{c}{2\sqrt{\pi} t^{3/2} Q_{zc}^4}[2ztN_{zc}(c^2+z^2+t^2-Q_{zc}) - P_{zc}M_{zc}(c^2+z^2+t^2+Q_{zc})]\end{aligned} \tag{A10}$$

$$\int_0^\infty \xi^{3/2} e^{-\xi z} J_1(\xi c) J_{1/2}(\xi t)\, d\xi = \frac{c}{\sqrt{\pi} t^{1/2} Q_{zc}^3}(2ztN_{zc} + P_{zc}M_{zc}) \tag{A11}$$

$$\int_0^\infty \xi^{5/2} e^{-\xi z} J_1(\xi c) J_{1/2}(\xi t)\, d\xi = \frac{2c}{\sqrt{\pi} t^{1/2} Q_{zc}^5}\{-tN_{zc}[(c^2+z^2+t^2)(c^2-5z^2+t^2)-4c^2t^2] + 2zM_{zc}[(c^2+z^2+t^2)(c^2+z^2-2t^2) + 2c^2t^2]\} - \frac{c}{2\sqrt{\pi} t^{3/2} Q_{zc}^4}[P_{zc}N_{zc}(c^2+z^2+t^2-Q_{zc}) + 2ztM_{zc}(c^2+z^2+t^2+Q_{zc})] \tag{A12}$$

$$\int_0^\infty I_0(\xi c)\, e^{-\xi t} \cos(\xi s)\, d\xi = \frac{M_{sc}}{\sqrt{2} Q_{sc}} \tag{A13}$$

$$\int_0^\infty \xi I_0(\xi c)\, e^{-\xi t} \cos(\xi s)\, d\xi = \frac{1}{\sqrt{2} Q_{sc}^3}[-s(c^2+z^2+t^2)N_{sc} + t(-c^2+s^2+t^2)M_{sc}] \tag{A14}$$

$$\int_0^\infty \xi I_1(\xi c)\, e^{-\xi t} \cos(\xi s)\, d\xi = -\frac{c}{\sqrt{2} Q_{sc}^3}(2stN_{sc} + P_{sc}M_{sc}) \tag{A15}$$

$$\int_0^\infty I_1(\xi c)\, e^{-\xi t} \sin(\xi s)\, d\xi = \frac{1}{\sqrt{2} c Q_{sc}}(tN_{sc} - sM_{sc}) \tag{A16}$$

$$\int_0^\infty \xi I_1(\xi c)\, e^{-\xi t} \sin(\xi s)\, d\xi = \frac{c}{\sqrt{2} Q_{sc}^3}(2stM_{sc} - P_{sc}N_{sc}) \tag{A17}$$

$$\int_0^\infty \xi I_0(\xi c)\, e^{-\xi t} \sin(\xi s)\, d\xi = \frac{1}{\sqrt{2} Q_{sc}^3}[t(-c^2+s^2+t^2)N_{sc} + s(c^2+s^2+t^2)M_{sc}] \tag{A18}$$

$$\int_0^\infty \frac{1}{\xi} K_0(\xi c) \sinh(\xi t) \cos(\xi s)\, d\xi = \frac{\pi}{4} \arcsin\left[\frac{\sqrt{2}}{c^2}(tN_{sc} - sM_{sc})\right] \tag{A19}$$

$$\int_0^\infty \frac{1}{\xi} K_1(\xi c) \sinh(\xi t) \sin(\xi s)\, d\xi = \frac{\pi M_{sc}}{2\sqrt{2} c} \tag{A20}$$

$$\int_0^\infty \xi K_0(\xi c) \sinh(\xi t) \cos(\xi s)\, d\xi = \frac{\pi}{2\sqrt{2} Q_{sc}^3}[tN_{sc}(c^2-s^2-t^2) - sM_{sc}(c^2+s^2+t^2)] \tag{A21}$$

$$\int_0^\infty K_1(\xi c) \sinh(\xi t) \cos(\xi s)\, d\xi = \frac{\pi}{2\sqrt{2} c Q_{sc}}(tN_{sc} - sM_{sc}) \tag{A22}$$

$$\int_0^\infty K_0(\xi c) \cosh(\xi t) \cos(\xi s)\, d\xi = \frac{\pi N_{sc}}{2\sqrt{2} Q_{sc}} \tag{A23}$$

$$\int_0^\infty \xi K_1(\xi c) \cosh(\xi t) \cos(\xi s)\, d\xi = \frac{\pi c}{2\sqrt{2} Q_{sc}^3}(P_{sc}N_{sc} - 2stM_{sc}) \tag{A24}$$

$$\int_0^\infty \xi K_1(\xi c) \sinh(\xi t) \sin(\xi s)\, d\xi = \frac{\pi c}{2\sqrt{2} Q_{sc}^3}(2stN_{sc} + P_{sc}M_{sc}) \tag{A25}$$

$$\int_0^\infty K_0(\xi c) \sinh(\xi t) \sin(\xi s)\, d\xi = \frac{\pi M_{sc}}{2\sqrt{2} Q_{sc}} \tag{A26}$$

$$\int_0^\infty K_1(\xi c) \cosh(\xi t) \sin(\xi s)\, d\xi = \frac{\pi}{2\sqrt{2} c Q_{sc}}(sN_{sc} + tM_{sc}) \tag{A27}$$

$$\int_0^\infty \xi K_0(\xi c) \cosh(\xi t) \sin(\xi s)\, d\xi = \frac{\pi}{2\sqrt{2} Q_{sc}^3}[sN_{sc}(c^2+s^2+t^2) + tM_{sc}(c^2-s^2-t^2)]. \tag{A28}$$

The identities given below in eqns (A29)–(A35) are derived with the aid of Oberhettinger[10].

$$\int_0^\infty x I_0(ax) K_0(xy) \sin(bx)\, dx = \frac{b}{[b^2+(a+y)^2]^{1/2}[b^2+(a-y)^2]} E(k) \tag{A29}$$

$$\int_0^\infty x^2 I_0(ax) K_1(xy) \sin(bx)\, dx = \frac{b}{[b^2+(a+y)^2]^{1/2}[b^2+(a-y)^2]}\left\{\left[\frac{2(a+y)}{b^2+(a+y)^2} - \frac{2(a-y)}{b^2+(a-y)^2} - \frac{1}{2y}\right] E(k) + \left[\frac{1}{2y} - \frac{(a+y)}{b^2+(a+y)^2}\right] K(k)\right\} \tag{A30}$$

$$\int_0^\infty x^2 I_1(ax) K_0(xy) \sin(bx)\, dx = \frac{b}{[b^2+(a+y)^2]^{1/2}[b^2+(a-y)^2]}\left\{\left[\frac{1}{2a} - \frac{2(a+y)}{b^2+(a+y)^2} - \frac{2(a-y)}{b^2+(a-y)^2}\right] E(k) - \left[\frac{1}{2a} - \frac{(a+y)}{b^2+(a+y)^2}\right] K(k)\right\} \tag{A31}$$

$$\int_0^\infty x^2 I_0(ax) K_0(xy) \cos(bx)\, dx = \frac{1}{[b^2+(a+y)^2]^{1/2}[b^2+(a-y)^2]}\left\{\left[1 - \frac{2b^2}{b^2+(a+y)^2} - \frac{2b^2}{b^2+(a-y)^2}\right] E(k) + \frac{b^2}{b^2+(a+y)^2} K(k)\right\} \tag{A32}$$

$$\int_0^\infty x^2 I_1(ax)K_1(xy)\cos(bx)\,dx = \frac{1}{2a[b^2+(a+y)^2]^{1/2}[b^2+(a-y)^2]}\left\{\left[\frac{a^2+y^2}{y}+\frac{4ab^2}{b^2+(a+y)^2}-\frac{4ab^2}{b^2+(a-y)^2}\right]E(k) - \left[\frac{a(a-y)}{y}+\frac{(a+y)(b^2-a^2+y^2)}{b^2+(a+y)^2}\right]K(k)\right\} \quad \text{(A33)}$$

$$\int_0^\infty xI_1(ax)K_0(xy)\cos(bx)\,dx = \frac{1}{2a[b^2+(a+y)^2]^{1/2}}\left\{\left[\frac{b^2-a^2+y^2}{b^2+(a-y)^2}\right]E(k)-K(k)\right\} \quad \text{(A34)}$$

$$\int_0^\infty xI_0(ax)K_1(xy)\cos(bx)\,dx = -\frac{1}{2y[b^2+(a+y)^2]^{1/2}}\left[\frac{b^2+a^2-y^2}{b^2+(a-y)^2}\right]E(k)-K(k)\Big\} \quad \text{(A35)}$$

where

$$k = \frac{2(ay)^{1/2}}{[b^2+(a+y)^2]^{1/2}}. \quad \text{(A36)}$$

Eason *et al.*[16] provided some integral identities enabling the derivation of the following identities given in eqns (A37)–(A48).

$$\int_0^\infty \xi\, e^{-2h\xi}J_0(\xi t)J_1(\xi r)\,d\xi = \frac{1}{r\pi[(t+r)^2+4h^2]^{1/2}}\left\{\frac{r^2-t^2-4h^2}{(t-r)^2+4h^2}E(\theta)+K(\theta)\right\} \quad \text{(A37)}$$

$$\int_0^\infty \xi^2 e^{-2h\xi}J_0(\xi t)J_1(\xi r)\,d\xi = \frac{2h}{r\pi[(t+r)^2+4h^2]^{3/2}[(t-r)^2+4h^2]}\left\{\frac{(r^2-t^2)(7r^2+t^2)+8h^2(3r^2-t^2-2h^2)}{(t-r)^2+4h^2}E(\theta) - (r^2-t^2-4h^2)K(\theta)\right\} \quad \text{(A38)}$$

$$\int_0^\infty \xi^3 e^{-2h\xi}J_0(\xi t)J_1(\xi r)\,d\xi = -\frac{1}{r\pi[(t+r)^2+4h^2]^{5/2}[(t-r)^2+4h^2]^3}\{[(r^2-t^2)^3(7r^2+t^2)-4h^2(r^2-t^2)(23r^4+74t^2r^2-t^4) - 16h^4(65r^4-46t^2r^2-3t^4)-64h^6(33r^2-5t^2)+512h^8]E(\theta) - [(t-r)^2+4h^2][(r^2-t^2)^3-48h^2r^2(r^2-t^2)-16h^4(11r^2-3t^2)+128h^6]K(\theta)\} \quad \text{(A39)}$$

$$\int_0^\infty \xi\, e^{-2h\xi}J_1(\xi t)J_1(\xi r)\,d\xi = \frac{2h}{tr\pi[(t+r)^2+4h^2]^{1/2}}\left\{\frac{t^2+r^2+4h^2}{(t-r)^2+4h^2}E(\theta)-K(\theta)\right\} \quad \text{(A40)}$$

$$\int_0^\infty \xi^2 e^{-2h\xi}J_1(\xi t)J_1(\xi r)\,d\xi = -\frac{1}{tr\pi[(t+r)^2+4h^2]^{3/2}[(t-r)^2+4h^2]}\left\{\frac{(t^4-r^4)(t^2-r^2)+8h^2(t^4-6t^2r^2+r^4)+16h^4(t^2+r^2)}{(t-r)^2+4h^2}E(\theta) - [(t^2-r^2)^2+4h^2(t^2+r^2)]K(\theta)\right\} \quad \text{(A41)}$$

$$\int_0^\infty \xi^3 e^{-2h\xi}J_1(\xi t)J_1(\xi r)\,d\xi = -\frac{2h}{tr\pi[(t+r)^2+4h^2]^{5/2}[(t-r)^2+4h^2]^3}\{[3(t^2-r^2)^2(t^4+14t^2r^2+r^4)+4h^2(t^2+r^2)(9t^4-50t^2r^2+9r^4) + 16h^4(9t^4-74t^2r^2+9r^4)+192h^6(t^2+r^2)]E(\theta) - [(t-r)^2+4h^2][3(t^2+r^2)(t^2-r^2)^2+8h^2(3t^2-r^2)(t^2-3r^2)+48h^4(t^2+r^2)]K(\theta)\} \quad \text{(A42)}$$

$$\int_0^\infty \xi\, e^{-2h\xi}J_0(\xi t)J_0(\xi r)\,d\xi = \frac{4h}{\pi[(t+r)^2+4h^2]^{1/2}[(t-r)^2+4h^2]}E(\theta) \quad \text{(A43)}$$

$$\int_0^\infty \xi^2 e^{-2h\xi}J_0(\xi t)J_0(\xi r)\,d\xi = -\frac{2}{\pi}\left\{\frac{(t^2-r^2)^2-8h^2(t^2+r^2)-48h^4}{[(t+r)^2+4h^2]^{3/2}[(t-r)^2+4h^2]^2}E(\theta)+\frac{4h^2}{[(t+r)^2+4h^2]^{3/2}[(t-r)^2+4h^2]}K(\theta)\right\} \quad \text{(A44)}$$

$$\int_0^\infty \xi^3 e^{-2h\xi}J_0(\xi t)J_0(\xi r)\,d\xi = -\frac{4h}{\pi[(t+r)^2+4h^2]^{5/2}[(t-r)^2+4h^2]^3}\{4[3(t^4-r^4)(t^2-r^2)+h^2(13t^4-58t^2r^2+13r^4)-40h^4(t^2+r^2) - 176h^6]E(\theta)-[(t-r)^2+4h^2][3(t^2-r^2)^2-8h^2(t^2+r^2)-80h^4]K(\theta)\} \quad \text{(A45)}$$

$$\int_0^\infty \xi\, e^{-2h\xi}J_1(\xi t)J_0(\xi r)\,d\xi = \frac{1}{t\pi[(t+r)^2+4h^2]^{1/2}}\left\{\frac{t^2-r^2-4h^2}{(t-r)^2+4h^2}E(\theta)+K(\theta)\right\} \quad \text{(A46)}$$

$$\int_0^\infty \xi^2 e^{-2h\xi}J_1(\xi t)J_0(\xi r)\,d\xi = \frac{2h}{t\pi[(t+r)^2+4h^2]^{3/2}[(t-r)^2+4h^2]}\left\{\frac{(t^2-r^2)(7t^2+r^2)+8h^2(3t^2-r^2-2h^2)}{(t-r)^2+4h^2}E(\theta) - (t^2-r^2-4h^2)K(\theta)\right\} \quad \text{(A47)}$$

$$\int_0^\infty \xi^3 e^{-2h\xi}J_1(\xi t)J_0(\xi r)\,d\xi = -\frac{1}{t\pi[(t+r)^2+4h^2]^{5/2}[(t-r)^2+4h^2]^3}\{[(t^2-r^2)^3(7t^2+r^2)-4h^2(t^2-r^2)(23t^4+74t^2r^2-r^4) - 16h^4(65t^4-46t^2r^2-3r^4)-64h^6(33t^2-5r^2)+512h^8]E(\theta) - [(t-r)^2+4h^2][(t^2-r^2)^3-48h^2t^2(t^2-r^2)-16h^4(11t^2-3r^2)+128h^6]K(\theta)\} \quad \text{(A48)}$$

where

$$\theta = \left[\frac{4tr}{(t+r)^2+4h^2}\right]^{1/2}. \quad \text{(A49)}$$

The following integral identities are reproduced here from Ref.[15] to facilitate the determination of the singular behavior at the upper end of shell and rod:

$$\int_0^\infty \frac{x^{s-1}}{(1+x^2)}\sin(ax)\,dx = \frac{1}{2}\pi\sec\left(\frac{1}{2}s\pi\right)\sinh a+\frac{1}{2}\Gamma(s)\sin\left(\frac{1}{2}\pi s\right)[e^{-a}e^{i(1-s)\pi}\gamma(1-s,-a)-e^{a}\gamma(1-s,a)] \quad \text{(A50)}$$

$$\int_0^\infty \frac{x^{s-t}}{(1+x^2)} \cos(ax)\,dx = \frac{1}{2}\pi csc\left(\frac{1}{2}s\pi\right)\cosh a + \frac{1}{2}\Gamma(s)\cos\left(\frac{1}{2}\pi s\right)[e^{-a}\,e^{i(1-s)\pi}\gamma(1-s,-a) - e^{a}\gamma(1-s,a)] \quad \text{(A51)}$$

where

$$\gamma(p,x) = \int_0^x t^{p-1} e^{-t}\,dt = p^{-1}x^{1/2p-1/2}\,e^{-1/2x}M_{1/2p-1/2,\,1/2p}(x) \quad \text{(A52)}$$

$$\int_0^\infty t^{-3/4} e^{-1/2at} M_{\alpha,-1/4}(at)\,e^{-pt}\,dt = \pi^{1/2}\left(\frac{a}{p}\right)^{1/4} p^{\alpha}(p+a)^{-\alpha-1/4} \quad \text{(A53)}$$

$$\int_0^\infty t^{-1/4} e^{-1/2at} M_{\alpha,1/4}(at)\,e^{-pt}\,dt = \frac{1}{2}\pi^{1/2}\left(\frac{a}{p}\right)^{3/4} p^{\alpha}(p+a)^{-\alpha-3/4}. \quad \text{(A54)}$$